

Controlling the False Split Rate in Tree-Based Aggregation

Simeng Shao, Jacob Bien, Adel Javanmard*

Data Sciences and Operations, University of Southern California

August 12, 2021

Abstract

In many domains, data measurements can naturally be associated with the leaves of a tree, expressing the relationships among these measurements. For example, companies belong to industries, which in turn belong to ever coarser divisions such as sectors; microbes are commonly arranged in a taxonomic hierarchy from species to kingdoms; street blocks belong to neighborhoods, which in turn belong to larger-scale regions. The problem of tree-based aggregation that we consider in this paper asks which of these tree-defined subgroups of leaves should really be treated as a single entity and which of these entities should be distinguished from each other.

We introduce the *false split rate*, an error measure that describes the degree to which subgroups have been split when they should not have been. We then propose a multiple hypothesis testing algorithm for tree-based aggregation, which we prove controls this error measure. We focus on two main examples of tree-based aggregation, one which involves aggregating means and the other which involves aggregating regression coefficients. We apply this methodology to aggregate stocks based on their volatility and to aggregate neighborhoods of New York City based on taxi fares.

Keywords: Multiple testing, false discovery rate, rare features, hierarchy

1 Introduction

A common challenge in data modeling is striking the right balance between models that are sufficiently flexible to adequately describe the phenomenon being studied and those that are simple enough to be easily interpretable. We consider this tradeoff within the increasingly common context in which data measurements can be associated with the leaves of a known

*A. Javanmard is partially supported by the Sloan Research Fellowship in mathematics, an Adobe Data Science Faculty Research Award and the NSF CAREER Award DMS-1844481. J. Bien was supported in part by NIH Grant R01GM123993 and NSF CAREER Award DMS-1653017.

tree. Such data structures arise in myriad domains from business to science, including the classification of occupations (US OMB 2018), businesses (US OMB 2017), products, geographic areas, and taxonomies in ecology.

Measurements in low-level branches of the tree may share a lot in common, and so—in the absence of evidence to the contrary—a data modeler would favor a simpler (literally “high-level”) description in which distinctions within low-level branches would not be made; on the other hand, when there is evidence of a difference between sibling branches, then modeling them as distinct from each other may be warranted. We use the term *tree-based aggregation* to refer to the process of deciding which branches’ leaves should be treated as the same (i.e., aggregated) and which should be treated as different from each other (i.e. split apart).

Tree-based aggregation procedures have been proposed in various contexts, including regression problems, in which features represent counts of rare events (Yan & Bien 2020) or counts of microbial species (Bien et al. 2021), and in graphical modeling (Wilms & Bien 2021). These approaches focus on prediction and estimation but do not address the hypothesis testing question of whether a particular split should occur.

We formulate the general tree-based aggregation problem as a multiple testing problem involving a parameter vector θ^* whose elements correspond to leaves of a known tree. Our goal is to partition the leaves based on branches of the tree so that the set of parameters in each group share the same value. Every non-leaf node has an associated null hypothesis that states that all of its leaves have the same parameter value. Type I errors correspond to splitting up groups unnecessarily; type II errors correspond to aggregating groups with different parameter values.

In Section 2, we define an error measure, called the *false split rate* (FSR), that corresponds to the fraction of splits made that were unnecessary. Within our tree-based setting, we show that controlling the FSR is related to controlling the false discovery rate (Benjamini & Hochberg 1995), with equivalence in the special case of a binary tree.

In Section 3, we propose a tree-based aggregation procedure that leverages this connection. Our algorithm proceeds in a top-down fashion, only testing hypotheses of nodes whose parents were rejected. Such an approach to hierarchical testing originates with Yekutieli (2008), which lays the foundation for the multiple testing problem on trees. Our procedure is closely related to more recent work by Lynch & Guo (2016), which increases power using carefully chosen node-specific thresholds that depend on where the hypothesis is located in the hierarchy. This work was in turn further developed in Ramdas et al. (2017). Other work involving various forms of a hierarchy-based multiple testing problem (although not having to do with aggregation in the sense of this paper) include Bogomolov et al. (2017), Heller et al. (2018), Katsevich & Sabatti (2019). While these works focus on FDR control, another line of work uses hierarchical testing for gradually locating non-zero variables while controlling the family-wise error rate (Meinshausen 2008, Guo et al. 2019).

In Section 4, we consider two concrete scenarios where tree-based aggregation is natural. In the first scenario, the parameter vector θ^* represents the mean of a scalar signal measured on the leaves of the tree. In the second scenario, θ^* is a (potentially high-dimensional) vector

of regression coefficients where features are associated with leaves of the tree.

Finally, we demonstrate through simulation studies (Section 5) and real data experiments (Section 6) the empirical merits of our framework and algorithm. We consider two applications, corresponding to the two concrete scenarios of tree-based aggregation. The first application involves aggregation of stocks (with respect to the NAICS’s sector-industry tree) based on mean log-volatility. The second application aggregates neighborhoods of New York City (with respect to a geographically based hierarchy) based on a regression vector for predicting taxi drivers’ monthly total fares based on the frequency of different starting locations.

Notation: For an integer p , we write $[p] = \{1, 2, \dots, p\}$. For $a, b \in \mathbb{R}$, we write $a \wedge b$ and $a \vee b$ for their minimum and maximum, respectively. We use \mathbf{e}_i to denote the i -th standard basis vector. For $\mathbf{x} \in \mathbb{R}^p$, we define $\|\mathbf{x}\|_q = \left(\sum_{j=1}^p |x_j|^q\right)^{1/q}$ for $q \geq 0$. For a set $S \subseteq [p]$, $\mathbf{x}_S = (x_i)_{i \in S}$ is the vector obtained by restricting the vector \mathbf{x} to the indices in set S . We use the term “tree” throughout to denote a rooted directed tree. Given a tree \mathcal{T} with leaf set \mathcal{L} , we write \mathcal{T}_u for the subtree rooted at $u \in \mathcal{T}$ and \mathcal{L}_u for its leaf set.

2 Problem setup

2.1 A multiple hypothesis testing formulation for aggregation

Let \mathcal{T} be a known tree with p leaves, each corresponding to a coordinate of the unobserved parameter vector $\boldsymbol{\theta}^* \in \mathbb{R}^p$. We formulate the tree-aggregation task as a multiple hypothesis testing problem: To each internal (non-leaf) node u of the tree we assign a null hypothesis

$$\mathcal{H}_u^0 : \text{All elements of } \boldsymbol{\theta}_{\mathcal{L}_u}^* \text{ have the same value,} \tag{1}$$

where $\boldsymbol{\theta}_{\mathcal{L}_u}^*$ is the subvector of $\boldsymbol{\theta}^*$ restricted to leaves of the subtree rooted at u . Rejecting the null hypothesis \mathcal{H}_u^0 implies that the leaves under u should be further split into smaller groups. Given the way the hypotheses are defined, a logical constraint to impose on the output of a testing procedure is the following:

Constraint 1. *The parent of a rejected node must itself be rejected.*

By constraint 1, the set of rejected nodes will then form a subtree \mathcal{T}_{rej} of \mathcal{T} (sharing the same root as \mathcal{T}), and furthermore the subtrees rooted at the leaves of \mathcal{T}_{rej} represent the aggregated groups. Our goal is to develop testing procedures that result in high quality splits of the parameters. In order to measure the performance of an aggregation (or equivalently a set of splits) we propose a new criterion as follows.

False Split Rate (FSR). Recall that we are interested in splits that can be expressed as a combination of branches of the tree \mathcal{T} . Therefore if we order the leaves (from left to right), if two leaves are in the same group, then the other leaves between them are also in the same group. For partitioning an ordered sequence of p leaves, we have $p - 1$ potential positions for

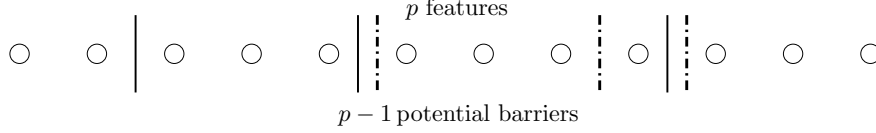


Figure 1: An example of leaves partition. There are $p = 12$ leaves in total, hence 11 potential barriers. The solid barriers indicate the true splitting of leaves, while the dashed barriers result in the achieved splitting of leaves. In terms of the vector of barriers, $\text{FDP}^b = \frac{1}{3}$ and $\text{TPP}^b = \frac{2}{3}$. In terms of splitting of leaves, $\text{FSP} = \frac{5-4}{4-1} = \frac{1}{3}$ and power $= 1 - \frac{5-4}{4-1} = \frac{2}{3}$.

the barriers of groups. We use a vector $\boldsymbol{\vartheta} \in \{0, 1\}^{p-1}$ to denote whether the corresponding barrier exists at that position. Each realization of such vector will result in a unique splitting of leaves, and vice versa. Let $\boldsymbol{\vartheta}^*$ and $\widehat{\boldsymbol{\vartheta}}$ respectively denote the corresponding vectors for the true splitting \mathcal{C}^* and an achieved splitting $\widehat{\mathcal{C}}$. In Figure 1 we give an example of $p = 12$ leaves. The solid barriers mark the true splitting, $\boldsymbol{\vartheta}^* = (0, 1, 0, 0, 1, 0, 0, 0, 1, 0, 0)$; the dashed barriers mark the achieved splitting, $\widehat{\boldsymbol{\vartheta}} = (0, 0, 0, 0, 1, 0, 0, 1, 1, 0, 0)$.

We can view the splitting task as a barrier discovery problem. The false discovery proportion and true positive proportion can then be written as

$$\text{FDP}^b := \frac{|\{j \in [p-1] : \vartheta_j^* = 0, \widehat{\vartheta}_j = 1\}|}{|\{j \in [p-1] : \widehat{\vartheta}_j = 1\}|}, \quad \text{TPP}^b := \frac{|\{j \in [p-1] : \vartheta_j^* = 1, \widehat{\vartheta}_j = 1\}|}{|\{j \in [p-1] : \vartheta_j^* = 1\}|}. \quad (2)$$

Since a set of barriers determines certain splitting of the leaves, we can express the above quantity in terms of the resulting groups. Suppose $\widehat{\mathcal{C}} = \{\widehat{C}_1, \dots, \widehat{C}_M\}$ is a splitting of the leaves $[p]$, and $\mathcal{C}^* = \{C_1^*, \dots, C_K^*\}$ is the true splitting. For each true group C_i^* , $i \in \{1, \dots, K\}$, we count the number of splits of C_i^* by members of $\widehat{\mathcal{C}}$, i.e., $\sum_{j=1}^M \mathbb{1}\{C_i^* \cap \widehat{C}_j \neq \emptyset\} - 1$. Therefore, the total number of excessive (false) splits of C_i^* is given by

$$\sum_{i=1}^K \left(\sum_{j=1}^M \mathbb{1}\{C_i^* \cap \widehat{C}_j \neq \emptyset\} - 1 \right) = \sum_{i=1}^K \left(\sum_{j=1}^M \mathbb{1}\{C_i^* \cap \widehat{C}_j \neq \emptyset\} \right) - K,$$

while the total number of splits is $(M-1) \vee 1$. We define the *false split proportion* (FSP) and true positive proportion (interchanging \mathcal{C}^* and $\widehat{\mathcal{C}}$) as

$$\text{FSP} := \frac{\sum_{i=1}^K \left(\sum_{j=1}^M \mathbb{1}\{C_i^* \cap \widehat{C}_j \neq \emptyset\} \right) - K}{(M-1) \vee 1}, \quad \text{TPP} := 1 - \frac{\sum_{i=1}^M \left(\sum_{j=1}^K \mathbb{1}\{C_i^* \cap \widehat{C}_j \neq \emptyset\} \right) - M}{K-1}. \quad (3)$$

In the next lemma, we prove that the quantities FSP and TPP in terms of groups are equivalent to quantities FDP^b and TPP^b for the barrier discovery problem.

Lemma 2.1. *For the quantities FSP and TPP, given by (3), and the quantities FDP^b and TPP^b , given by (2), the following holds true: $\text{FSP} = \text{FDP}^b$, $\text{TPP} = \text{TPP}^b$.*

We refer to Appendix B.1 for the proof of Lemma 2.1. The *false split rate* (FSR) and the expected power are defined as

$$\text{FSR} := \mathbb{E}(\text{FSP}), \quad \text{Power} := \mathbb{E}(\text{TPP}), \quad (4)$$

where the expectation is with respect to the randomness in $\widehat{\mathcal{C}}$, which in our context will depend on the p -values for the hypotheses of the form (1). In the next section we provide another characterization for FSR in the tree-aggregation context, and in Section 3 we develop a testing procedure that controls FSR at a pre-specified level $\alpha < 1$.

2.2 FSR on a tree

While the FSR metric can be calculated for a general splitting of p objects using definition (3), in this section we focus on splittings that can be expressed as a combination of branches of \mathcal{T} as explained in the previous section. We will provide an equivalent characterization of FSP in this context in terms of specific structural properties of \mathcal{T} .

For a testing procedure satisfying Constraint 1, the rejected nodes on the tree still maintain the tree structure. We use \mathcal{T}_{rej} to represent the subtree of rejected nodes on the tree \mathcal{T} . We also define $\text{deg}_{\mathcal{T}}(u)$ as the (out) degree of node u on tree \mathcal{T} (the number of children of node u); similarly, $\text{deg}_{\mathcal{T}_{\text{rej}}}(u)$ is the degree of node u on the subtree \mathcal{T}_{rej} . We use \mathcal{F} as the set of false rejections in \mathcal{T} . Lastly, we define \mathcal{B}^* as the set of nodes whose leaf sets correspond to the true aggregation, i.e., \mathcal{B}^* is such that $\mathcal{C}^* = \{\mathcal{L}_u \mid u \in \mathcal{B}^*\}$. This characterization of \mathcal{C}^* stems from the assumption that the true aggregation is among the partitions allowed by the tree.

Our next lemma characterizes the number of false splits and the total number of splits in terms of the tree \mathcal{T} and its subtree \mathcal{T}_{rej} . By virtue of this lemma we have an alternative characterization of FSP (and FSR), which is more amenable to analysis.

Lemma 2.2. *Define V and R as follows:*

$$V := \sum_{u \in \mathcal{F}} \left(\text{deg}_{\mathcal{T}}(u) - \text{deg}_{\mathcal{T}_{\text{rej}}}(u) \right) - |\mathcal{B}^* \cap \mathcal{F}|, \quad R := \max \left\{ \sum_{u \in \mathcal{T}_{\text{rej}}} \left(\text{deg}_{\mathcal{T}}(u) - \text{deg}_{\mathcal{T}_{\text{rej}}}(u) \right) - 1, 0 \right\}. \quad (5)$$

Then V and R quantify the number of false splits and the total number of splits, respectively. Consequently, we have $\text{FSP} = V/R$ and $\text{FSR} = \mathbb{E}(V/R)$, where FSP and FSR are defined as in (3) and (4).

A key quantity in the above characterization is $\text{deg}_{\mathcal{T}}(u) - \text{deg}_{\mathcal{T}_{\text{rej}}}(u)$, which counts the number of additional splits due to rejecting \mathcal{H}_u^0 . Figure 2 represents a concrete example to illustrate the quantities and the equivalence stated in the lemma.

Remark. *Let us stress that the FSP metric in general can be very different from the standard FDR metric for multiple hypothesis testing. FDR measures the overall performance of the testing rule, including the hypotheses at the inner nodes, while FSR concerns the quality*

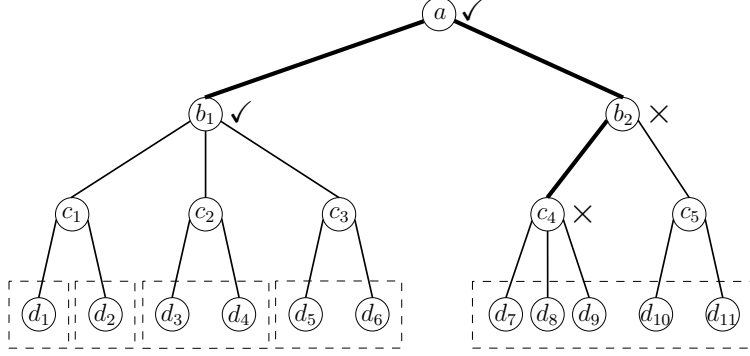


Figure 2: An example of \mathcal{T} , in which dashed boxes show the true aggregation of the leaves, \mathcal{C}^* , into $K = 5$ groups, with $\mathcal{B}^* = \{d_1, d_2, c_2, c_3, b_2\}$. The thicker edges and the nodes they connect form \mathcal{T}_{rej} , with \checkmark 's marking true rejections and \times 's marking false rejections \mathcal{F} . The rejections correspond to an achieved aggregation with $M = 7$ groups: $\{d_1, d_2\}, \{d_3, d_4\}, \{d_5, d_6\}, \{d_7\}, \{d_8\}, \{d_9\}, \{d_{10}, d_{11}\}$. On the right branch of the tree, two false rejections lead to a nonzero false split rate, $\text{FSP} = \frac{8-5}{7-1} = \frac{3}{6}$. We have $V = (3 - 0) + (2 - 1) - 1 = 3$, and $R = (2 - 2) + (3 - 0) + (2 - 1) + (3 - 0) - 1 = 6$. Hence $\frac{V}{R} = \text{FSP}$. On the left branch of the tree, there is one missing rejection (c_1) that leads to a true positive proportion of $\text{TPP} = 1 - \frac{8-7}{5-1} = \frac{3}{4}$.

of the splitting of the leaves. Therefore, methods for controlling FDR on trees cannot be applied to control FSR (as shown numerically in Section 5.2). That said, we show in the next lemma that FSP and FDP become equivalent for the special case of a binary tree.

The following corollary states the equivalence for the special case in which \mathcal{T} is a binary tree. In this case, FSP corresponds exactly to the commonly used FDP, which is the ratio between the number of false rejections and the total number of rejections.

Lemma 2.3. *For a binary tree, the quantities V and R given by (5) can be simplified as $V = |\mathcal{F}|$ and $R = |\mathcal{T}_{\text{rej}}|$. Therefore, $\text{FSP} = |\mathcal{F}| / |\mathcal{T}_{\text{rej}}|$ and $\text{FSR} = \text{FDR} := \mathbb{E}(|\mathcal{F}| / |\mathcal{T}_{\text{rej}}|)$.*

We defer the proofs for Lemma 2.2 and Lemma 2.3 to Appendix B.

3 Hierarchical aggregation testing with FSR control

So far we have defined the metric FSR to measure the quality of a splitting of leaves and proposed an alternate characterization of it in terms of the structure of the rejected (and false rejected) nodes as in Lemma 2.2. In this section, we introduce a new multiple testing procedure to test the null hypotheses \mathcal{H}_u^0 , starting from the root and proceeding down the tree. The procedure assumes that each non-leaf node u has a p -value that is super-uniform under \mathcal{H}_u^0 , i.e.

$$\mathbb{P}(p_u \leq t) \leq t \quad \text{for all } t \in [0, 1]. \quad (6)$$

Later, in Section 4, we discuss how to construct such p -values for two statistical applications.

We call our multiple testing procedure **HAT**, shorthand for *hierarchical aggregation testing*, as the parameters in the returned splits can be aggregated together to improve model interpretability and in some cases improve the predictive power of the model. The **HAT** procedure controls the FSR both for independent p -values (Section 3.1) and under arbitrary dependence of the p -values (Section 3.2).

The hypotheses defined in (1) are indeed intersection hypotheses, i.e.,

$$\mathcal{H}_u^0 \text{ holds} \Rightarrow \mathcal{H}_v^0 \text{ holds for } \forall v \in \mathcal{T}_u, \quad (7)$$

where \mathcal{T}_u is the subtree rooted at node u . In other words, the parent of a non-null node must be non-null, and if a node is null then every child of it is null as well. This property motivates us to use a top-down sequential testing algorithm on the tree that honors Constraint 1.

Before describing the **HAT** algorithm, we establish some notation. We sometimes write $\mathcal{H}_{d,u}^0$ to make it explicit that node u is at depth d of the tree, where the depth of a node is one plus the length of the unique path that connects the root to that node (the root is at depth 1). We also use \mathcal{T}^d for the set of non-leaf nodes at depth d of \mathcal{T} .

The testing procedure runs as follows. Let α be our target FSR level. Starting from the root node, at each level d we only test hypotheses at the nodes whose parents are rejected. The test levels for hypotheses are determined by a step-up threshold function so that the test level at each hypothesis $\mathcal{H}_{d,u}^0$ depends on the number of leaves under this node $|\mathcal{L}_u|$, the target level α , the maximum node degree denoted by Δ , and the number of splits made in previous levels, denoted by $R^{1:(d-1)}$. The details of our **HAT** procedure are given in Algorithm 1, and depend on node-specific thresholds $\alpha_u(r)$, both explicitly and through the function

$$R^d(r) := \sum_{u \in \mathcal{T}^d} \mathbb{1}\{p_u \leq \alpha_u(r)\}(\deg_{\mathcal{T}}(u) - 1). \quad (8)$$

Algorithm 1 *Hierarchical Aggregation Testing (HAT) Algorithm*

Require: : FSR level α , Tree \mathcal{T} , p -values p_u for $u \in \mathcal{T} \setminus \mathcal{L}$.

Ensure: : Aggregation of leaves such that the procedure controls FSR.

initialize $\mathcal{T}_{\text{rej}}^1 = \{\text{root}\}$, $R^{1:1} = \deg_{\mathcal{T}}(\text{root}) - 1$.

1: **repeat**

2: From depth $d = 2$ to maximum depth D of the tree \mathcal{T} , perform hypothesis testing on each node in \mathcal{T}^d . Compute r_d^* as

$$r_d^* = \max \{r \geq 0 : r \leq R^d(r)\},$$

where $R^d(r)$ is defined in (8), with threshold function $\alpha_u(r)$ given by (9) (for case of independent p -values) or (12) (under general dependence among p -values). Reject the nodes in the set $\mathcal{T}_{\text{rej}}^d = \{u \in \mathcal{T}^d : p_u \leq \alpha_u(r_d^*)\}$.

3: Update $\mathcal{T}_{\text{rej}}^{1:d} = \mathcal{T}_{\text{rej}}^{1:(d-1)} \cup \mathcal{T}_{\text{rej}}^d$, and $R^{1:d} = R^{1:(d-1)} + r_d^*$.

4: **until** No node in the current depth has a rejected parent or $d = D$.

3.1 Testing with independent p -values

Assuming that the node p -values p_u are independent, the threshold function $\alpha_u(r)$ used for testing $\mathcal{H}_{d,u}^0$ is defined as:

$$\alpha_u(r) = \mathbb{1}\{\text{parent}(u) \in \mathcal{T}_{\text{rej}}^{d-1}\} \frac{1}{\Delta} \frac{\alpha |\mathcal{L}_u| (R^{1:(d-1)} + r)}{p(1 - \frac{1}{\Delta^2}) \bar{h}_{d,r} + \alpha |\mathcal{L}_u| (R^{1:(d-1)} + r)}, \quad (9)$$

where $\bar{h}_{d,r}$ is the partial harmonic sum given by

$$\bar{h}_{d,r} = 1 + \sum_{m=R^{1:(d-1)}+r+1}^{p-1 - (\sum_{u \in \mathcal{T}^d} \deg_{\mathcal{T}}(u) - |\mathcal{T}^d| - r)} \frac{1}{m}. \quad (10)$$

Theorem 3.1. *Consider a tree with maximum node degree Δ and suppose that for each node u in the tree, under the null hypothesis \mathcal{H}_u^0 , the p -value p_u is super-uniform (see (6)). Further, assume that the p -values for the null nodes are independent from each other and from the non-null p -values. Then using Algorithm 1 with threshold function (9) to test intersection hypotheses \mathcal{H}_u^0 controls FSR under the target level α .*

The proof of Theorem 3.1 is given in Section A.1 of the appendix and uses a combination of different ideas. At the core of the proof is a ‘leave-one-out’ technique to decouple the quantities V and R . We also use the following *self-consistency* property of the testing rule. Observe that $R^d(r)$ counts the additional splits of the leaves that result due to the rejected nodes in depth d , assuming that the threshold level $\alpha_u(r)$ is used. We prove that the following self-consistency property holds: $R^d(r_d^*) = r_d^*$ where r_d^* is defined in Step 2 of Algorithm 1. In words, using r_d^* to test the nodes in \mathcal{T}^d (node u to be tested at level $\alpha_u(r_d^*)$) gives us r_d^* additional splits of the leaves, and therefore the update rule for $R^{1:d}$ in line 3 of the algorithm ensures that this quantity counts the number of splits formed from testing nodes in depth $1, \dots, d$. Using the self-consistency property and the leave-one-out technique, along with intricate probabilistic bounds in terms of structural properties of \mathcal{T} , we prove that FSR is controlled at the pre-assigned level α .

A few remarks are in order regarding the testing threshold $\alpha_u(r)$. From its definition, we have $\alpha_u(r) = 0$ if the parent hypothesis of u is not rejected. Also note that since the testing is done in a downward manner, the event $\{\text{parent}(u) \in \mathcal{T}_{\text{rej}}^{d-1}\}$ is observed by the time the node u is tested. Also note that as we reject more hypotheses early on, the burden of proof reduces for the subsequent hypotheses, because $\alpha_u(r)$ is increasing in $R^{1:(d-1)}$. This trend is similar to FDR control methods (e.g., Benjamini & Hochberg (1995), Javanmard & Montanari (2018b)). We also observe that $\alpha_u(r)$ is increasing in $|\mathcal{L}_u|$. For the nodes at upper levels of the tree, this is crucially useful as $R^{1:(d-1)}$ is small for these nodes, while $|\mathcal{L}_u|$ is large and compensates for it in the threshold function.

Our next theorem is a generalization of Theorem 3.1 to the case that the null p -values distribution deviates from a super-uniform distribution. We will use Theorem 3.2 to control FSR in Section 4.2 where we aim to aggregate the features in a linear regression setting. As

we will discuss, for this application we suggest to construct the p -values using a debiasing approach, which results in p -values that are asymptotically super-uniform (as the sample size n diverges).

Theorem 3.2. *Consider a tree with maximum node degree Δ and suppose that for each non-leaf node u in the tree, under the null hypothesis \mathcal{H}_u^0 , the p -value p_u satisfies $\mathbb{P}(p_u \leq t) \leq t + \varepsilon_0$ for all $t \in [0, 1]$, for a constant $\varepsilon_0 > 0$. Further, assume that the p -values for the null nodes are independent from each other and from the non-null p -values. Consider running Algorithm 1 to test intersection hypotheses \mathcal{H}_u^0 with the threshold function given by*

$$\alpha_u(r) = \mathbb{1}\{\text{parent}(u) \in \mathcal{T}_{\text{rej}}^{d-1}\} \left\{ \frac{1}{\Delta} \frac{\alpha|\mathcal{L}_u|(R^{1:(d-1)} + r)}{p(1 - \frac{1}{\Delta^2})\bar{h}_{d,r} + \alpha|\mathcal{L}_u|(R^{1:(d-1)} + r)} - \varepsilon_0 \right\}. \quad (11)$$

Then, FSR is controlled under the target level α .

3.2 Testing with arbitrarily dependent p -values

Theorems 3.1 and 3.2 assume that the null p -values are independent from each other and from the non-null p -values. To handle arbitrarily dependent p -values, we propose a modified threshold function:

$$\alpha_u(r) = \mathbb{1}\{\text{parent}(u) \in \mathcal{T}_{\text{rej}}^{d-1}\} \frac{\alpha|\mathcal{L}_u| \cdot \beta_d(R^{1:(d-1)} + r)}{p(\Delta - \frac{1}{\Delta})(D - 1)}, \quad (12)$$

where $\beta_d(\cdot)$ is a reshaping function of the form

$$\beta_d(R^{1:(d-1)} + r) = \frac{R^{1:(d-1)} + r}{\sum_{\substack{u \in \mathcal{T}^d \\ k=d(\delta-1)}} \deg_{\mathcal{T}}(u) \frac{1}{k}}, \quad (13)$$

and δ is the minimum node degree in $\mathcal{T} \setminus \mathcal{L}$. It is straightforward to see that the reshaping function is lowering the test thresholds compared to the independent p -values case, making the testing procedure more conservative to handle general dependence among p -values. In the next theorem, we show that with the reshaped testing threshold FSR is controlled for arbitrarily dependent p -values.

Theorem 3.3. *Consider a tree with maximum node degree Δ and minimum node degree δ , and suppose that for each node u in the tree, under the null hypothesis \mathcal{H}_u^0 , the p -value is super-uniform, i.e., (6) holds. The p -values for the nodes can be arbitrarily dependent. Then, HAT (Algorithm 1) with the reshaped threshold (12) controls FSR under the target level α .*

The proof of Theorem 3.3 builds upon a lemma from Blanchard & Roquain (2008) on dependency control of a pair of non-negative random variables. We refer to Section A.3 of the appendix for further details and the complete proof.

We conclude this section with an analogous result to Theorem 3.3, where the p -values are *approximately* super-uniform. This can also be perceived as a generalization of Theorem 3.2 to the case of arbitrarily dependent p -values.

Theorem 3.4. Consider a tree with maximum node degree Δ and minimum node degree δ , and suppose that for each non-leaf node u in the tree, under the null hypothesis \mathcal{H}_u^0 , the p -value p_u satisfies

$$\mathbb{P}(p_u \leq t) \leq t + \varepsilon_0, \quad \text{for all } t \in [0, 1],$$

for a constant $\varepsilon_0 > 0$. The p -values for the nodes can be arbitrarily dependent. Consider running Algorithm 1 to test the hypotheses \mathcal{H}_u^0 with threshold function given by

$$\alpha_u(r) = \mathbb{1}\{\text{parent}(u) \in \mathcal{T}_{\text{rej}}^{d-1}\} \left\{ \frac{\alpha |\mathcal{L}_u| \cdot \beta_d(R^{1:(d-1)} + r)}{p(\Delta - \frac{1}{\Delta})(D - 1)} - \varepsilon_0 \right\}, \quad (14)$$

with the reshaping function $\beta_d(\cdot)$ defined by (12). Then, FSR is controlled under the target level α .

Proof of Theorem 3.4 is similar to the proof of Theorem 3.3, and is deferred to Section A.3.1 of the appendix.

4 Two statistical applications

Here we consider two statistical applications of tree-based aggregation. In Section 4.1, we study the problem of testing equality of means, for which the nodewise p -values are formed by one-way ANOVA tests. In Section 4.2 we study the problem of aggregating features with the same coefficients in a linear regression setting.

4.1 Testing equality of means

In this application, we imagine that θ^* is a vector of unknown means and that at each leaf node i of a tree \mathcal{T} there is a noisy observation of the corresponding mean: $y_i = \theta_i^* + \varepsilon_i$, where the $\varepsilon_i \sim \mathbf{N}(0, \sigma^2)$ are independent. Given the y_i , we want to aggregate the leaves by testing the equality of their means. For each node $u \in \mathcal{T}$, we construct a p -value based on a one-way ANOVA test with known $\sigma > 0$,

$$p_u = 1 - F_{\chi_{\Delta_u-1}^2} \left(\sigma^{-2} \sum_{v \in \text{child}(u)} |\mathcal{L}_v| (\bar{y}_v - \bar{y}_u)^2 \right), \quad (15)$$

where $\bar{y}_v = |\mathcal{L}_v|^{-1} \sum_{i \in \mathcal{L}_v} y_i$, and $\text{child}(u)$ is the set of children of u . Also $\Delta_u := \deg_{\mathcal{T}}(u) = |\text{child}(u)|$ and $F_{\chi_{\Delta_u-1}^2}$ is the cdf of a $\chi_{\Delta_u-1}^2$ random variable. We show in the following lemma that the above construction gives bona fide p -values for our testing procedure.

Lemma 4.1. The p -value defined in (15) is uniform under \mathcal{H}_u^0 in (1). Furthermore, for any two distinct nodes $a, b \in \mathcal{T} \setminus \mathcal{L}$, p_a and p_b are independent.

Recall that the nodewise hypotheses $\{\mathcal{H}_u^0\}_{u \in \mathcal{T} \setminus \mathcal{L}}$ are intersection hypotheses as in (7), and therefore one can apply Simes' procedure to form bona fide intersection p -values.

The Simes' p -value at node a is given by $p_{a, \text{Simes}} := \min_{1 \leq k \leq |\mathcal{T}_a \setminus \mathcal{L}_a|} (p_{(k)} \cdot |\mathcal{T}_a \setminus \mathcal{L}_a|) / k$, where $p_{(k)}$ is the k th smallest p -value in $\mathcal{T}_a \setminus \mathcal{L}_a$. As shown by Simes (1986), as the original p -values are independent (as per Lemma 4.1), the Simes' p -values constructed as above are super-uniform, and hence can be used to test the nodewise hypotheses. However, note that the Simes' p -values are not independent anymore, so when applying the HAT procedure, we need to use the reshaped threshold function (12).

4.2 Testing equality of regression coefficients

Consider a linear model where the response variables are generated as $\mathbf{y} \sim \mathbf{N}(\mathbf{X}\boldsymbol{\theta}^*, \sigma^2 \mathbf{I}_n)$.

In many applications the features are counts data, i.e., X_{ij} records the frequency of an event j occurring in observation i . Yan & Bien (2020) note that when events rarely occur, a common practice is to remove the rare features in a pre-processing step; however, they show that when a tree is available, rare features can instead be aggregated to create informative predictors that count the frequency of tree-based unions of events. While Yan & Bien (2020) focused on predictive performance, here we focus on aggregation recovery itself by controlling FSR. To do so, we use the point estimator of Yan & Bien (2020), along with a debiasing approach to construct the nodewise p -values for our proposed testing procedure.

The Yan & Bien (2020) point estimator is the solution to the optimization problem,

$$\hat{\boldsymbol{\theta}} \in \arg \min_{\boldsymbol{\theta} \in \mathbb{R}^p} \frac{1}{2n} \|\mathbf{y} - \mathbf{X}\boldsymbol{\theta}\|_2^2 + \min_{\boldsymbol{\gamma} \in \mathbb{R}^{|\mathcal{T}|}} \lambda \left(\nu \sum_{u \in \mathcal{T} \setminus \text{root}} |\gamma_u| + (1 - \nu) \sum_{j=1}^p |\theta_j| \right) \quad \text{s.t. } \boldsymbol{\theta} = \mathbf{A}\boldsymbol{\gamma}, \quad (16)$$

where $\mathbf{A} \in \mathbb{R}^{p \times |\mathcal{T}|}$ encodes the tree structure with A_{ij} indicating whether leaf i is a descendant of node j . The resulting $\hat{\boldsymbol{\theta}}$ tends to be constant on branches of the tree, leading to aggregated features.

4.2.1 Constructing p -values for the null hypotheses

A challenge in constructing p -values for the null hypotheses \mathcal{H}_u^0 given in (1) is that the distribution of the estimator $\hat{\boldsymbol{\theta}}$ is not tractable. Moreover, due to the regularization term, this estimator is biased. We therefore use a debiasing approach.

The debiasing approach was pioneered in Javanmard & Montanari (2014), Zhang & Zhang (2014), van de Geer et al. (2014), Javanmard & Montanari (2018a) for statistical inference in high-dimensions where the sample size is much smaller than the dimension of the features (i.e., $n \ll p$). Regularized estimators such as the lasso (Tibshirani 1996) are popular point estimators in these regimes however they are biased. The focus of the debiasing work has been on statistical inference on individual model parameters, namely constructing p -values for null hypotheses of the form $\mathcal{H}_{0,i} : \theta_i^* = 0$. The debiasing approach has been extended for inference on linear functions of model parameters (Cai et al. 2017, 2019b) and

also general functionals of them (Javanmard & Lee 2020). The original debiasing method can also be used to perform inference on a group of model parameters, e.g. constructing valid p -values for null hypothesis $\mathcal{H}_0 : \boldsymbol{\theta}_A = 0$ where the group size $|A|$ is fixed as $n, p \rightarrow \infty$ (see e.g, Javanmard & Montanari (2014, Section 3.4)). More recently, Guo et al. (2019) have studied the group inference problem for linear regression model by considering sum-type statistics. Namely, by considering quadratic form hypotheses, $\mathcal{H}_0 : \boldsymbol{\theta}_A^\top \mathbf{G} \boldsymbol{\theta}_A = 0$, for a positive definite matrix \mathbf{G} . They propose a debiasing approach to directly estimate the quadratic form $\boldsymbol{\theta}_A^\top \mathbf{G} \boldsymbol{\theta}_A$ and to provide asymptotically valid p -values for the corresponding hypotheses. The constructed p -values are valid for any group size in terms of type-I error control. This work also discusses how by a direct application of the methodology developed in Meinshausen (2008), one can test significance of multiple groups, where the groups are defined by a tree structure. The method of Meinshausen (2008) is based on a hierarchical approach to test variables' importance. At the core, it constructs hierarchical adjusted p -values to account for the multiplicity of testing problems and controls the family wise error rate at the prespecified level. At every level of the tree, the p -value adjustment is a weighted Bonferroni correction and across different levels it is a sequential procedure with no correction but with the constraint that if a parent hypothesis is not rejected then the procedure does not go further down the tree. By comparison, our HAT algorithm controls the FSR, a very different criterion than the family wise error rate. Also HAT does not do any adjustment to p -values, and instead chooses the threshold levels in a sequential manner depending on the previous rejections and the structural properties of the tree.

Here we follow the methodology of Guo et al. (2019) to construct valid p -values for the HAT procedure, using the point estimator (16). We write \mathcal{H}_u^0 equivalently as $\tilde{\mathcal{H}}_u^0 : Q_u := \boldsymbol{\theta}_{\mathcal{L}_u}^{*\top} \mathbf{G}_u \boldsymbol{\theta}_{\mathcal{L}_u}^* = 0$, where \mathbf{G}_u is the centering matrix and we use the shorthand $\boldsymbol{\theta}_u := \boldsymbol{\theta}_{\mathcal{L}_u}$. To make inference on the quadratic form Q_u , we first consider the point estimator estimator $\hat{Q}_u := \hat{\boldsymbol{\theta}}_u^\top \mathbf{G}_u \hat{\boldsymbol{\theta}}_u$, where $\hat{\boldsymbol{\theta}}$ is the estimator given by (16). To debias \hat{Q}_u we first decompose the error term into

$$\hat{Q}_u - Q_u = \hat{\boldsymbol{\theta}}_u^\top \mathbf{G}_u \hat{\boldsymbol{\theta}}_u - \boldsymbol{\theta}_u^{*\top} \mathbf{G}_u \boldsymbol{\theta}_u^* = 2\hat{\boldsymbol{\theta}}_u^\top \mathbf{G}_u (\hat{\boldsymbol{\theta}}_u - \boldsymbol{\theta}_u^*) - (\hat{\boldsymbol{\theta}}_u - \boldsymbol{\theta}_u^*)^\top \mathbf{G}_u (\hat{\boldsymbol{\theta}}_u - \boldsymbol{\theta}_u^*).$$

The dominating term in this decomposition is $2\hat{\boldsymbol{\theta}}_u^\top \mathbf{G}_u (\hat{\boldsymbol{\theta}}_u - \boldsymbol{\theta}_u^*)$. The approach in Guo et al. (2019) is to develop an *unbiased* estimate of this term and then subtract this estimate from \hat{Q}_u . Given a projection direction $\hat{\mathbf{b}}$, the unbiased estimate is of the form

$$\frac{1}{n} \hat{\mathbf{b}}^\top \mathbf{X}^\top (\mathbf{y} - \mathbf{X} \hat{\boldsymbol{\theta}}) = \hat{\mathbf{b}}^\top \hat{\boldsymbol{\Sigma}} (\boldsymbol{\theta}^* - \hat{\boldsymbol{\theta}}) + \frac{1}{n} \hat{\mathbf{b}}^\top \mathbf{X}^\top \boldsymbol{\varepsilon},$$

where $\hat{\boldsymbol{\Sigma}} := \frac{1}{n} \mathbf{X}^\top \mathbf{X}$. The idea is to find a projection direction $\hat{\mathbf{b}}$ such that $\hat{\mathbf{b}}^\top \hat{\boldsymbol{\Sigma}} (\hat{\boldsymbol{\theta}} - \boldsymbol{\theta}^*)$ is a good estimate for $\hat{\boldsymbol{\theta}}_u^\top \mathbf{G}_u (\hat{\boldsymbol{\theta}}_u - \boldsymbol{\theta}_u^*)$. The projection direction $\hat{\mathbf{b}}$ is constructed by solving the following optimization problem:

$$\hat{\mathbf{b}} = \arg \min_{\mathbf{b}} \mathbf{b}^\top \hat{\boldsymbol{\Sigma}} \mathbf{b} \quad \text{s.t.} \quad \max_{\boldsymbol{\omega} \in \mathcal{C}_u} \left| \langle \boldsymbol{\omega}, \hat{\boldsymbol{\Sigma}} \mathbf{b} - [\hat{\boldsymbol{\theta}}_u^\top \mathbf{G}_u \quad \mathbf{0}]^\top \rangle \right| \leq \|\mathbf{G}_u \hat{\boldsymbol{\theta}}_u\|_2 \lambda_n, \quad (17)$$

where

$$\mathcal{C}_u = \left\{ \mathbf{e}_1, \dots, \mathbf{e}_p, \frac{1}{\|\mathbf{G}_u \widehat{\boldsymbol{\theta}}_u\|_2} [\widehat{\boldsymbol{\theta}}_u^\top \mathbf{G}_u \ \mathbf{0}]^\top \right\}$$

and λ_n is chosen to be of order $\sqrt{\log(p)/n}$. Finally the debiased estimator for Q_u is constructed as $\widehat{Q}_u^{\text{d}} := \widehat{\boldsymbol{\theta}}_u^\top \mathbf{G}_u \widehat{\boldsymbol{\theta}}_u + \frac{2}{n} \widehat{\mathbf{b}}^\top \mathbf{X}^\top (\mathbf{y} - \mathbf{X} \widehat{\boldsymbol{\theta}})$. Suppose that the true model $\boldsymbol{\theta}^*$ is s_0 sparse (i.e., it has s_0 nonzero entries). As shown in (Guo et al. 2019, Theorem 2), under the condition $s_0(\log p)/\sqrt{n} \rightarrow 0$, and assuming that the initial estimator $\widehat{\boldsymbol{\theta}}$ satisfies $\|\widehat{\boldsymbol{\theta}} - \boldsymbol{\theta}^*\|_2 \leq C\sqrt{s_0(\log p)/n}$ and $\|\widehat{\boldsymbol{\theta}} - \boldsymbol{\theta}^*\|_1 \leq Cs_0\sqrt{(\log p)/n}$ for some constant $C > 0$, then the residual $\widehat{Q}_u^{\text{d}} - Q_u$ asymptotically admits a Gaussian distribution. More specifically, $\widehat{Q}_u^{\text{d}} - Q_u = Z_u + \Delta_u$ where

$$Z_u \sim \mathbf{N}(0, \text{Var}(\widehat{Q}_u^{\text{d}})), \quad \text{Var}(\widehat{Q}_u^{\text{d}}) = \frac{4\sigma^2 \widehat{\mathbf{b}}^\top \widehat{\boldsymbol{\Sigma}} \widehat{\mathbf{b}}}{n}. \quad (18)$$

In addition, for any constant $c_1 > 0$, there exists a constant $c_2 > 0$ depending on c_1 such that

$$\mathbb{P} \left(|\Delta_u| \geq c_1 (\|\mathbf{G}_u \widehat{\boldsymbol{\theta}}_u\|_2 + \|\mathbf{G}_u\|_2) \frac{s_0 \log p}{n} \right) \leq 2pe^{-c_2 n}, \quad (19)$$

The above bound state that with high probability the bias term Δ_u is of order $s_0(\log p)/n$, while $\text{Var}(\widehat{Q}_u^{\text{d}})$ is of order $1/n$. Therefore under the condition $s_0(\log p)/\sqrt{n} \rightarrow 0$ the noise term Z_u dominates the bias term Δ_u .¹

Note that $\text{Var}(\widehat{Q}_u^{\text{d}})$ involves the noise variance σ^2 (which is the same for all nodes u). Let $\widehat{\sigma}$ be a consistent estimate of σ . Then the variance of the debiased estimator \widehat{Q}_u^{d} is estimated by

$$\widehat{\text{Var}}_\tau(\widehat{Q}_u^{\text{d}}) = \frac{4\widehat{\sigma}^2 \widehat{\mathbf{b}}^\top \widehat{\boldsymbol{\Sigma}} \widehat{\mathbf{b}}}{n} + \frac{\tau}{n}, \quad (20)$$

for some positive fixed constant τ . The term τ/n is just to ensure that the estimated variance is at least of order $1/n$ (in the case of $\widehat{\mathbf{b}}^\top \widehat{\boldsymbol{\Sigma}} \widehat{\mathbf{b}} = 0$), and so it dominates the bias component of \widehat{Q}_u^{d} . The exact choice of τ does not matter in the large sample limit ($n \rightarrow \infty$).

Using this result, we construct the two-sided p -value for the null hypothesis $\widetilde{\mathcal{H}}_u^0$ as follows:

$$p_u = 2 \left[1 - \Phi \left(\frac{|\widehat{Q}_u^{\text{d}}|}{\sqrt{\widehat{\text{Var}}_\tau(\widehat{Q}_u^{\text{d}})}} \right) \right],$$

where Φ is the cdf of the standard normal distribution.

¹In Guo et al. (2019), the probability bound $pe^{-c_2 n}$ was further simplified to $p^{-c'}$ since $n \gtrsim \log p$ and assuming $n, p \rightarrow \infty$.

Proposition 4.2. Consider the asymptotic distributional characterization of \widehat{Q}_u^d given by (18) and (19). Let $\widehat{\sigma} = \widehat{\sigma}(\mathbf{y}, \mathbf{X})$ be an estimator of σ satisfying, for any fixed $\varepsilon > 0$,

$$\lim_{n \rightarrow \infty} \mathbb{P}\left(\left|\frac{\widehat{\sigma}}{\sigma} - 1\right| \geq \varepsilon\right) = 0.$$

Under the condition $s_0(\log p)/\sqrt{n} \rightarrow 0$, for any fixed arbitrarily small constant ε_0 (say 0.001), there exists $n_0 > 0$ such that for all $n > n_0$, $\mathbb{P}(p_u \leq t) \leq t + \varepsilon_0$, for all $t \in [0, 1]$.

We refer to Appendix B.5 for the proof of Proposition 4.2. By virtue of Proposition 4.2, the constructed p -values satisfy the assumption of Theorem 3.4 and therefore by running the HAT procedure we are able to control FSR under the target level.

5 Simulations

In this section, we conduct simulation studies (using the `simulator` R package Bien 2016) to understand the performance of HAT in different settings.

5.1 Testing on a binary tree with idealized p -values

Since FSR and FDR are equivalent in the special case of a binary tree (by Lemma 2.3), we begin by comparing HAT with a testing procedure proposed by Lynch & Guo (2016) to control FDR in the hierarchical testing context (For non-binary trees there is no such reference to compare with, since FSR is a criterion proposed by the present work, and there is no other algorithm in the literature to control FSR). Their method, which we refer to as LG, corresponds to Algorithm 1 with several modifications. First, their thresholds are given by

$$\alpha_u(r) = \alpha \frac{|\mathcal{L}_u(\widetilde{\mathcal{T}})|}{|\mathcal{L}_{\text{root}}(\widetilde{\mathcal{T}})|} \frac{m_u(\widetilde{\mathcal{T}}) + R^{1:(d-1)} + r - 1}{m_u(\widetilde{\mathcal{T}})}, \quad (21)$$

where $\widetilde{\mathcal{T}}$ is the tree in which we take \mathcal{T} and remove the leaves, $m_u(\widetilde{\mathcal{T}})$ is the number of descendants of node u in $\widetilde{\mathcal{T}}$, $|\mathcal{L}_u(\widetilde{\mathcal{T}})|$ is the number of leaves in $\widetilde{\mathcal{T}}$ that descend from u . Also, they initialize $R^{1:1} = 1$ and, instead of (8), they take $R^d(r) = \sum_{u \in \widetilde{\mathcal{T}}^d} \mathbb{1}\{p_u \leq \alpha_u(r)\}$.

We randomly generate p points from $\text{Unif}[0, 1]$ and form a binary tree structure among them using hierarchical clustering. We let $K = |\mathcal{B}^*|$ be the number of true groups by cutting the tree into K disjoint subtrees with the R function `cutree`. The nodes that are the roots of the subtrees form \mathcal{B}^* . All non-leaf nodes in \mathcal{B}^* and their non-leaf descendants are null nodes, and we generate their p -values independently from $\text{Unif}([0, 1])$. All ancestors of \mathcal{B}^* are non-null nodes, with p -values we generate independently from $\text{Beta}(1, 60)$.

For each pair of p and K , the set of p -values are simulated independently for 100 repetitions as described above. We calculate FSP and TPP based on the aggregation of leaves that results and average over the 100 values to estimate FSR and the mean power.

The left two panels of Figure 3 show how FSR and average power change with K when p is fixed at 1000. We can see that both methods control FSR under the target α 's. In terms

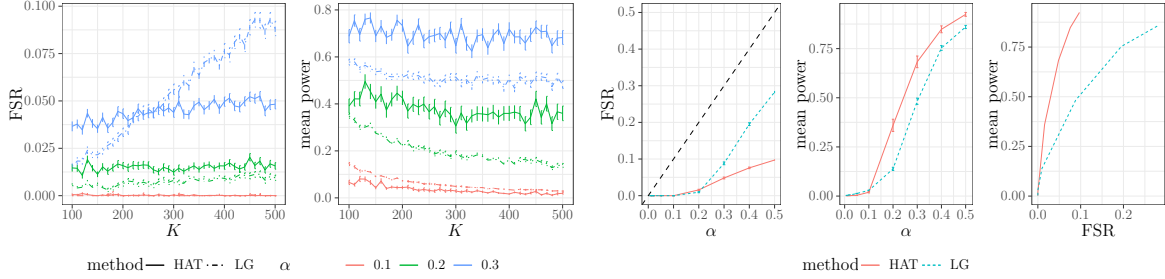


Figure 3: *Plots of achieved FSR and average power by our algorithm (HAT) and Lynch and Guo’s algorithm (LG), on a binary tree with $p = 1000$ leaves and independent p -values. For the right three panels, $K = 500$.*

of power, when $\alpha = 0.1$, the LG method enjoys slightly higher power. For larger α , however, the average power achieved by our HAT method is higher; the gap in power enlarges as K increases. When K is large with the tree fixed, meaning that the \mathcal{B}^* nodes are at deeper levels, LG’s power drops at a faster rate than ours. Indeed, for these α values, our method shows a substantial advantage when we have a deep tree and the non-null nodes appear at deeper levels of the tree.

The right three panels of Figure 3 show how achieved FSR and average power change with α in the setting where $p = 1000$, $K = 500$. We observe again that HAT achieves higher power than LG when α is above 0.1. From the left panel, we see that both methods are conservative in that the achieved FSR is lower than the target level α , but as evident from the right-most panel, HAT showcases a better tradeoff between FSR and the mean power.

5.2 Testing on a non-binary tree with idealized p -values

The LG algorithm is guaranteed to control FSR in the previous section due to the equivalence between FSR and FDR in the special case of a binary tree. However, for a non-binary tree, the LG algorithm does not have a theoretical guarantee on FSR control.

We generate a tree where the root has degree 5, and each child of the root is either a non-leaf node with degree 10 or is a leaf node; we vary the number of non-root non-leaf nodes from 1 to 4, which results in p ranging from 14 to 41. The number of true groups is fixed at 5, therefore the root is the only non-null node. We simulate p -values for the interior nodes in the same fashion as in Section 5.1: the p -values for null nodes are simulated independently from $\text{Unif}([0, 1])$ and the p -values for non-null nodes are simulated independently from $\text{Beta}(1, 60)$. An estimate of FSR is obtained by averaging FSP over 100 runs. The achieved FSR is shown in Figure 4. As expected, we observe that the HAT procedure controls FSR under each target α for all values of p , whereas the LG algorithm does not.

Therefore, for aggregating leaves in general settings where the tree can be beyond binary, only our algorithm provably controls FSR under the pre-specified level. This highlights the importance of using our approach, which has guaranteed FSR control for tree-based aggregation problems with non-binary trees.

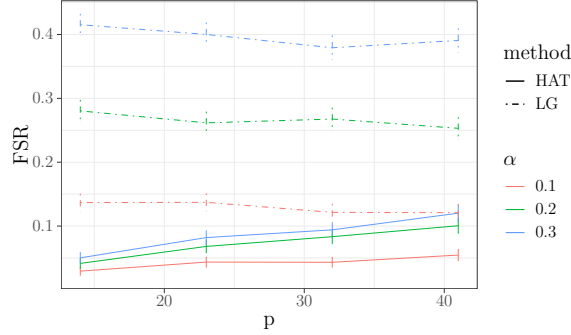


Figure 4: Plot of achieved FSR by HAT and LG on a non-binary tree with $K = 5$ and independent p -values. LG does not control FSR under the target levels.

5.3 Two statistical applications

5.3.1 Testing equality of means

In this section we apply the HAT procedure to the problem of testing equality of means. To simulate this setting, we form a balanced 3-regular tree with $p = 243$ leaves. For each K , we cut the tree into K disjoint subtrees, which leads to K non-overlapping subgroups of leaves. We assign a value to each leaf as $y_i = \theta_{k(i)}^* + \varepsilon_i$, $k(i) \in \{1, \dots, K\}$, $i \in \{1, \dots, p\}$, where $k(i)$ represents the group of leaf node i and the elements of θ are independently generated from a $\text{Unif}(1, 1.5)$ distribution multiplied by random signs, and ε_i 's from a $\text{N}(0, \sigma^2)$ distribution. We simulate 100 runs by generating 100 independent ε 's with the noise level set to $\sigma = 0.3$. The p -values are calculated as in (15).

By Lemma 4.1, the ANOVA p -values are independent. Thus, by Theorem 3.1, we can perform HAT using the using threshold function (9). Alternatively, we can form the bona fide p -value using Simes' procedure, and test with the reshaped threshold function that is designed for arbitrarily dependent p -values.

We calculate FSR and average power by taking the average of the FSP and power over the 100 runs. Figure 5 demonstrates how FSR and average power change with K . We observe that using Simes' p -values together with the reshaped thresholds achieves both lower FSR and higher power, which makes sense in this context because large effect sizes low in the tree may not translate to large effect sizes high in the tree.

5.3.2 Testing equality of regression coefficients

We apply HAT to the application of testing equality of regression coefficients. We assume a high-dimensional linear model as described in Section 4.2 and generate p coefficients that take K unique values. This partition comes from leaves of disjoint subtrees of \mathcal{T} . We compute the p -values using the debiased method on each node as in Section 4.2.1. The details of the data generating process are described in Section E of the appendix.

For each K , we simulate 100 independent ε 's. The initial estimator $\hat{\theta}$ that solves the optimization problem (16) is achieved by using the R package `rare` Yan & Bien (n.d.). The

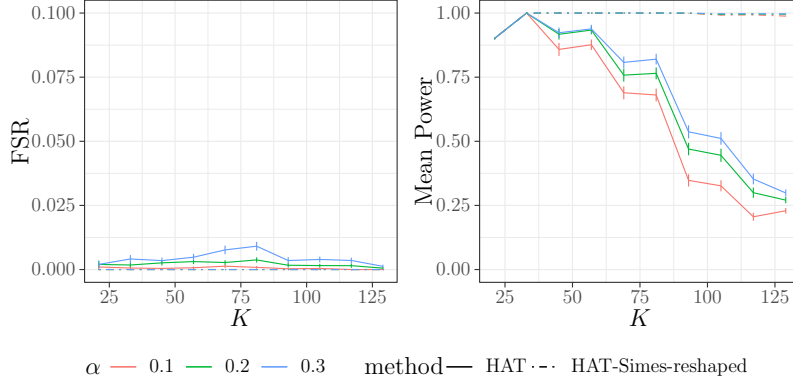


Figure 5: *Plots of achieved FSR and mean power with ANOVA p -values on a 3-regular tree ($p = 243, \sigma = 0.3$).*

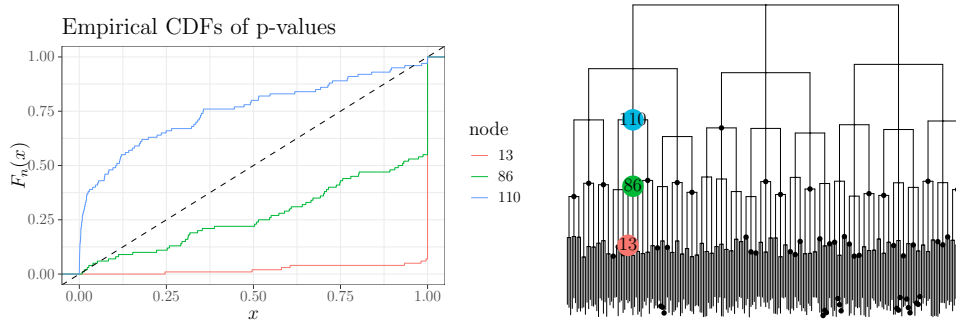


Figure 6: *Plots of empirical CDFs of three nodes under the setting $n = 100, p = 243, \beta = 0.6, K = 30, \rho = 0.2, \sigma = 0.6$. Node #110 is a non-null node, node #86 is a null node in \mathcal{B}^* , and node #13 is a null node that is a child of #86.*

tuning parameters λ and ν are chosen by cross-validation over a 2×10 grid. We then follow the steps described in Section 4.2.1 to compute the p -values at each node. The positive constant τ in (20) is set to one and the noise level estimate $\hat{\sigma}$ is obtained using the scaled lasso Sun & Zhang (2012) (R package `scalreg`).

Figure 6 shows the empirical cdf of the p -values, obtained from the 100 realizations of the noise, at three representative nodes when $K = 57$. Among the three nodes, node #110 is a non-null node, which means $\theta_{\mathcal{L}_{110}}^*$ contains at least two distinct values. Nodes #13 and #86 are both null nodes but at different depths on the tree. node #86 is one of the \mathcal{B}^* nodes and node #13 is a descendant of node #86. The curve of p -values at node #110 is above the diagonal line, which means the distribution has a higher density at small values than uniform distribution. On the contrary, the distribution of p -values at nodes #13 and #86 are super-uniform. The curve for a deeper level node seems to be further away from the diagonal line than its ancestor node.

The p -values generated are not necessarily independent, so we use the reshaped threshold

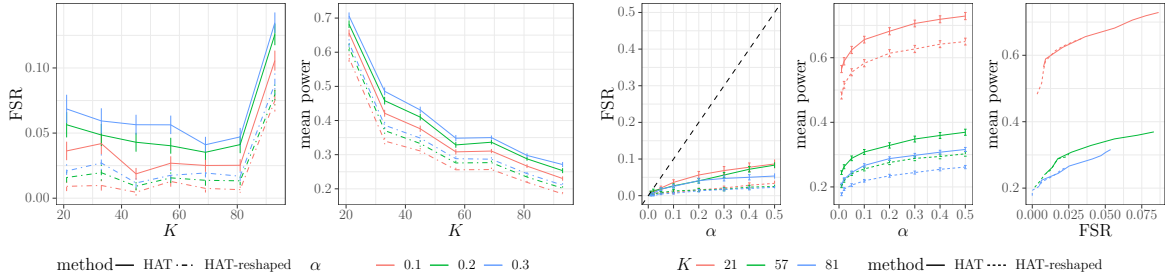


Figure 7: *Plots of the achieved FSR and average power on a 3-regular tree ($n = 100$, $p = 243$, $\beta = 0.6$, $\rho = 0.2$, $\sigma = 0.6$) and p -values generated by the debiasing procedure.*

function (12), which we have shown in theory controls FSR with arbitrarily dependent p -values. We also test with the threshold function (9), which we have not proven FSR control when the p -values are dependent. In Figure 7, we demonstrate the result for both threshold functions, varying K and α . We observe from the plots that testing with both threshold functions control FSR below each target level α . The reshaping function makes the threshold more conservative, hence the power of the HAT test with the reshaping function is generally lower.

6 Data examples

6.1 Application to stocks data

In this section, we analyze whether volatility of stocks is similar if companies are in similar categories. We use daily stock price data from January 1, 2015 to December 31, 2019, derived from the US Stock Database ©2021 Center for Research in Security Prices (CRSP), The University of Chicago Booth School of Business (CRSP Stocks 2015-2019). Specifically, we wish to aggregate stocks in a similar sector unless their volatility levels are significantly different. We use several criteria for screening stocks of interest: We only keep common stocks that are publicly traded throughout this entire period; we also avoid penny stocks that have prices under \$0.01 per share. After pre-screening, we have $n = 2538$ stocks in total. Following Parkinson (1980) and Martens & van Dijk (2007), we use the high-low range estimator for the daily variance $v_t = \frac{1}{4\log(2)}(\log(H_t) - \log(L_t))^2$, where H_t and L_t are day t 's highest and lowest prices, respectively. We take the average of v_t throughout the 5-year period as our estimate for the volatility of each stock and log-transform the volatility to reduce skewness.

We combine this stock log-volatility data with company industry classification information provided by the Compustat database (Compustat Industrial - Annual Data 2015-2019). The classification system we use is the North American Industry Classification System (NAICS), an industry classification system that employs a six digit code: the first two digits designate the largest sector; the third, fourth, fifth and sixth digits designate the subsector, industry group, industry, and national industry, respectively. We use this hierarchy to con-

struct a tree with the first six layers representing the digits and the last layer, namely the leaves, corresponding to the individual companies.

At every node on the tree, we acquire a p -value by performing an F -test (Equation 8.4, Seber & Lee 2012), for testing equality of the log-volatilities of all stocks within the subtree defined by this node. We further apply Simes’ procedure to the p -values. We use HAT with the reshaped thresholds and $\alpha = 0.4$. The achieved aggregation result is summarized in Table 1 in Section F of the appendix.

The final aggregation result consists of 40 clusters at a variety of levels: 21 at sector level, 8 at subsector level, 10 at industry group level, and one at company level. Two sectors “Manufacturing II” and “Finance and Insurance” are split into further clusters while other sectors remain undivided. Figure 8 focuses on the 347 companies in the subsector “Credit Intermediation and Related Activities”. Each point represents the log-volatility of a company. The three facets correspond to three industry groups within the subsector and eight levels on the y -axis correspond to the eight industries nested in the industry groups. As can be observed in the plot, the industry group “Depository Credit Intermediation” has significantly lower mean (around -8.27) compared to the other two industry groups in the subsector (around -7.67 and -7.59 respectively). Therefore, the null hypothesis that the three industry groups have similar mean volatility is rejected. On the contrary, within each industry group, there are no noticeable differences among different industries, leading none of the null hypotheses at the industry group level to be rejected.

6.2 Application to New York City (NYC) taxi data

We apply our method of aggregating features to the NYC Yellow Taxi Trip data (available at data.cityofnewyork.us), restricting attention to taxi trips made in December 2013. After cleaning the data, we have 13.5 million trips made by $n = 32704$ taxi drivers. We take the total fare each taxi driver earned as the response variable and take the number of rides starting from each of $p = 194$ neighborhood tabulation areas (NYC Planning 2020) as the features. We form a tree with NTAs as leaves, by connecting the root to five nodes, representing the boroughs of NYC. Within each borough, we apply hierarchical clustering to the NTAs based on their geographical coordinates. This results in a tree with depth 10. The availability of taxis is not uniformly distributed across the city (see Figure 10 of Section G of the appendix) and \mathbf{X} is a highly sparse matrix.

To aggregate neighborhood features, we perform the following procedure: with data \mathbf{X} and \mathbf{y} , as well as the given tree structure, we first fit the penalized regression (16) to construct an initial estimate of the coefficients $\hat{\boldsymbol{\theta}}$. The estimation is achieved by using the `rare` package with cross-validation across for choosing the regularization parameters ν and λ across a grid of 5×50 values. Next, we carry out the debiasing step by solving the optimization problem (17), with the R package `quadprog`. Note that the noise level σ is unknown, which we estimate by using the scaled lasso (Sun & Zhang 2012; R package `scalreg`). Moreover, the positive constant τ in (20) is set to one. After constructing the p -values for each non-leaf node of the tree, we run HAT with $\alpha = 0.3$.

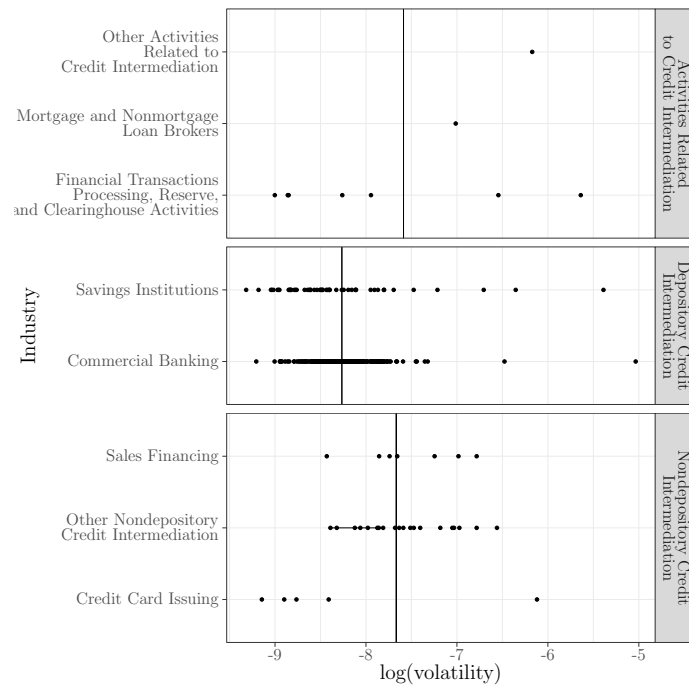
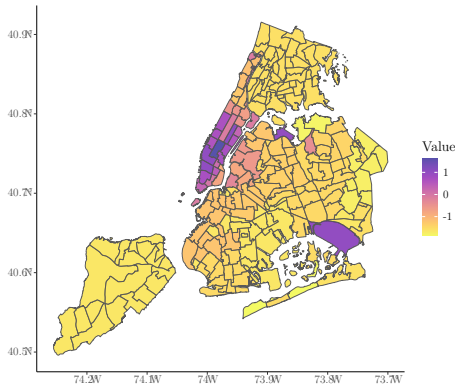


Figure 8: The subsector “Credit Intermediation and Related Activities” consists of 347 companies, represented as points. These fall into 3 industry groups and 8 industries. Applying HAT rejects the null hypothesis that the 3 industry groups have the same mean log-volatility, but does not reject this within each industry group.



Method	MSPE
L1	95.780
L1-dense	95.864
ls-boro	147.438
L1-agg-h	102.593
Rare	95.725
HAT (our method)	95.459

Figure 9: *Left: Map colored with log-transformed least square coefficients from regressing fare on features from HAT’s aggregation of neighborhoods of New York City. There are 44 aggregated clusters out of the 194 neighborhoods. Darker colors correspond to higher fitted coefficients. Right: Prediction performance of the 6 methods with the test data set.*

6.2.1 Aggregation results

Our testing result leads to 44 aggregated clusters, with the boroughs of Bronx and Staten Island remaining undivided. Brooklyn, Queens, and Manhattan are divided into 7, 14, and 21 subgroups, respectively. The left panel of Figure 9, we shows the coefficients resulting from performing least squares on these 44 aggregated features. Trips starting from Manhattan and parts of Queens, especially the airports, have higher coefficient values. Within Manhattan, areas like Hell’s kitchen, Times Square, and Penn Station have some of the higher coefficient values.

In Section G.1 of the appendix we show, by taking subsamples of different sizes, that reducing sample size leads to fewer rejections and therefore fewer aggregated groups.

6.2.2 Comparing prediction performance

In this section, we assess prediction performance achieved by our aggregated features. We hold out a random sample of 20% of the drivers as the test set, and train with the remaining 80%. We compare to the following models (each tuned via 10-fold cross validation):

- Lasso with the original variables (L1).
- Lasso with only dense features (L1-dense): We drop features with $< 0.5\%$ nonzeros then fit a lasso on the remaining 99 features.
- Least squares with clusters aggregated to the five boroughs (ls-boro).
- Lasso with clusters aggregated at optimized height (L1-agg-h). We tune (over a grid of 5 values) an extra parameter h that determines the aggregation height in the tree.

- Rare regression proposed by Yan & Bien (2020) (**Rare**).

We compute the mean squared prediction error (MSPE) of each method on the test set (see right panel of Figure 9). The **L1** and **L1-dense** methods are not aggregation-related and achieve similar performance. Both **ls-boro** and **L1-agg-h** achieve some level of aggregation but the aggregations are determined at certain heights. **L1-agg-h** has an additional tuning parameter and is therefore advantageous. Lastly, both **Rare** and our method achieve aggregation in a flexible way, and the prediction results are comparable. **Rare** selects 43 aggregation clusters while our method achieves 46 groups in total.

In Section G of the appendix, we perform an additional experiment with a synthetic response (but with \mathbf{X} and \mathcal{T} from this data set) to measure the FSR and power.

7 Conclusion

In many application domains, ranging from business and e-commerce, to computer vision and image processing, biology and ecology, the data measurements are naturally associated with the leaves of a tree which represents the data structure. Motivated by these applications, in this work we studied the problem of splitting the measurements into non-overlapping subgroups which can be expressed as a combination of branches of the tree. The subgroups ideally express the leaves that should be aggregated together, and perceived as single entities. We formulate the task of tree-based aggregation/splitting as a multiple testing problem and introduced a novel metric called false split rate which corresponds to the fraction of splits made that were unnecessary. In addition, we proposed a so called **HAT** procedure (and a few variants of it) to return a splitting of leaves, which is guaranteed to control the false split rate under the target level.

It is worth noting some of the salient distinctions of the setup considered in this paper with the classical hierarchical clustering. Firstly, in hierarchical clustering the tree is cut at a fixed level, while our framework allows for more flexible summarization of the tree where different branches are cut at different depths. In other words, our framework yields multi-scale resolution of the data. Secondly, the clustering problem is often formulated as an unsupervised problem. In contrast, our framework can be perceived as supervised clustering problem where the labeled data are used to group the leaves by combining the branches of the tree.

A Proof of main theorems

A.1 Proof of Theorem 3.1

Recall the definition of the quantities V and R :

$$V := \sum_{u \in \mathcal{F}} \left(\deg_{\mathcal{T}}(u) - \deg_{\mathcal{T}_{\text{rej}}}(u) \right) - |\mathcal{B}^* \cap \mathcal{F}|,$$

$$R := \max \left\{ \sum_{u \in \mathcal{T}_{\text{rej}}} \left(\deg_{\mathcal{T}}(u) - \deg_{\mathcal{T}_{\text{rej}}}(u) \right) - 1, 0 \right\}.$$

Note that $R > 0$ because $\mathcal{T}_{\text{rej}} \subset \mathcal{T}$ (recall that \mathcal{T}_{rej} does not include any leaves of \mathcal{T} as there is no hypothesis associated to those nodes.) As we showed in Lemma 2.2, the false split rate can be written in terms of V and R :

$$\text{FSR} = \mathbb{E} \left[\frac{V}{R \vee 1} \right].$$

For node $a \in \mathcal{B}^*$ let $\mathcal{F}_a = \mathcal{F} \cap \mathcal{T}_a$, and define the quantity V_a as follows:

$$V_a = \begin{cases} \sum_{u \in \mathcal{F}_a} \left(\deg_{\mathcal{T}}(u) - \deg_{\mathcal{T}_{a,\text{rej}}}(u) \right) - 1, & \text{if } \mathcal{F}_a \neq \emptyset \\ 0 & \text{otherwise} \end{cases} \quad (22)$$

By definition $V_a \geq 0$. Indeed, from the proof of Lemma 2.2, V_a is the number of false splits in the set \mathcal{L}_a . Also it is easy to verify that $V = \sum_{a \in \mathcal{B}^*} V_a$.

We first show that

$$\mathbb{E} \left(\frac{V_a}{R} \right) \leq \frac{\alpha |\mathcal{L}_a|}{p}, \quad \text{for } a \in \mathcal{B}^*. \quad (23)$$

Denote by $S(\mathcal{T}_a)$ the set of all nonempty subtrees of \mathcal{T}_a rooted at node a . We also let $V_a(\mathcal{T}')$ be the number of false splits in \mathcal{L}_a when the rejection subtree is \mathcal{T}' , i.e.,

$$V_a(\mathcal{T}') = \sum_{u \in \mathcal{T}'} \left(\deg_{\mathcal{T}}(u) - \deg_{\mathcal{T}'}(u) \right) - 1.$$

Here we used that $a \in \mathcal{B}^*$ and therefore any rejection in \mathcal{T}' is a false rejection and so $\mathcal{F}_a = \mathcal{T}'$. Define $\tilde{R}_{\mathcal{T}'}$ to be the total number of splits when we set $p_u = 0$ for $u \in \mathcal{T}'$ and $p_u = 1$ for $u \in \mathcal{T}_a \setminus \mathcal{T}'$.

Note that $\tilde{R}_{\mathcal{T}_{a,\text{rej}}} = R$ since for $u \in \mathcal{T}_{a,\text{rej}}$ the p -value p_u is already below the threshold at node u and for $u \in \mathcal{T}_a \setminus \mathcal{T}_{a,\text{rej}}$, p_u is already above the threshold at that node u . Therefore, writing $\mathcal{P}_{\mathcal{T}_a}^c = \{p_u : u \notin \mathcal{T}_a\}$, we have

$$\begin{aligned} \mathbb{E} \left[\frac{V_a}{R} \mathbb{1}(V_a > 0) \middle| \mathcal{P}_{\mathcal{T}_a}^c \right] &= \sum_{\mathcal{T}' \in S(\mathcal{T}_a)} \mathbb{E} \left[\frac{V_a(\mathcal{T}')}{\tilde{R}_{\mathcal{T}'}} \mathbb{1}(\mathcal{T}_{a,\text{rej}} = \mathcal{T}') \middle| \mathcal{P}_{\mathcal{T}_a}^c \right] \\ &= \sum_{\mathcal{T}' \in S(\mathcal{T}_a)} \frac{V_a(\mathcal{T}')}{\tilde{R}_{\mathcal{T}'}} \cdot \mathbb{P}(\mathcal{T}_{a,\text{rej}} = \mathcal{T}'), \end{aligned} \quad (24)$$

where $S(\mathcal{T}_a)$ denotes the set of all nonempty subtrees of \mathcal{T}_a rooted at node a , and we have used the fact that $V_a(\mathcal{T}')$ is non-random and $\tilde{R}_{\mathcal{T}'}$ is constant conditional on $\mathcal{P}_{\mathcal{T}_a}^c$.

Define $R^d(r) := \sum_{u \in \mathcal{T}^d} \mathbb{1}\{p_u \leq \alpha_u(r)\}(\deg_{\mathcal{T}}(u) - 1)$. Observe that $R^d(r_d^*)$ is the additional number of splits made by the rejected nodes in depth d , going from depth $d - 1$ to depth d , because the hypotheses \mathcal{H}_u^0 in depth d are tested at level $\alpha_u(r_d^*)$. Using our notation this can be written as the identity $R^{1:d} = R^{1:(d-1)} + R^d(r_d^*)$.

We argue that $r_d^* = R^d(r_d^*)$. To see why, note that by definition

$$r_d^* = \max \left\{ 0 \leq r \leq \sum_{u \in \mathcal{T}^d} \deg_{\mathcal{T}}(u) - |\mathcal{T}^d| : r \leq R^d(r) \right\}.$$

Hence, $r_d^* \leq R^d(r_d^*)$ and $r_d^* + 1 > R^d(r_d^* + 1)$. Since $R^d(r)$ is an integer valued function, the fact that $R^d(r_d^* + 1) < r_d^* + 1$ implies $R^d(r_d^* + 1) \leq r_d^*$. Thus, $r_d^* \leq R^d(r_d^*) \leq R^d(r_d^* + 1) \leq r_d^*$, which gives $r_d^* = R^d(r_d^*)$, and consequently

$$R^{1:d} = R^{1:(d-1)} + r_d^*. \quad (25)$$

We next continue by upper bounding the right hand side of (24). Based on our testing methodology, described in Algorithm 1, a typical node u at depth d is tested at level $\alpha_u(r_d^*)$ given by (9). We have

$$\begin{aligned} \alpha_u(r_d^*) &= \mathbb{1}\{\text{parent}(u) \in \mathcal{T}_{\text{rej}}^{d-1}\} \frac{1}{\Delta} \frac{\alpha |\mathcal{L}_u|(R^{1:(d-1)} + r_d^*)}{p(1 - \frac{1}{\Delta^2})\bar{h}_{d,r} + \alpha |\mathcal{L}_u|(R^{1:(d-1)} + r_d^*)} \\ &= \mathbb{1}\{\text{parent}(u) \in \mathcal{T}_{\text{rej}}^{d-1}\} \frac{1}{\Delta} \frac{\alpha |\mathcal{L}_u|R^{1:d}}{p(1 - \frac{1}{\Delta^2})\bar{h}_{d,r} + \alpha |\mathcal{L}_u|R^{1:d}} \\ &= \mathbb{1}\{\text{parent}(u) \in \mathcal{T}_{\text{rej}}^{d-1}\} \frac{1}{\Delta} \frac{\gamma_u}{p(1 - \frac{1}{\Delta^2}) + \gamma_u}, \end{aligned} \quad (26)$$

with

$$\gamma_u := \frac{\alpha}{\bar{h}_{d,r}} |\mathcal{L}_u|R^{1:d}.$$

Note that $\alpha_u(r_d^*)$ is increasing in γ_u .

Lemma A.1. *Suppose that $u \in \mathcal{T}_a$ and the node a is at level d_a . Then, on the event $\{\mathcal{T}_{a,\text{rej}} = \mathcal{T}'\}$ we have*

$$\gamma_u \leq \frac{\alpha}{\bar{h}_{d,r}} |\mathcal{L}_a| \tilde{R}_{\mathcal{T}'}. \quad (27)$$

The proof of Lemma A.1 follows readily from the fact that on the event $\{\mathcal{T}_{a,\text{rej}} = \mathcal{T}'\}$, we have $R^{1:d} \leq \tilde{R}_{\mathcal{T}'}$. Also, since $u \in \mathcal{T}_a$ we have $|\mathcal{L}_u| \leq |\mathcal{L}_a|$.

We next provide an upper bound for the thresholds $\alpha_u(r_d^*)$ for all nodes $u \in \mathcal{T}_{a,\text{rej}}$, which will be useful in controlling FSR. For positive integer m , define

$$\tilde{\gamma}_{a,m} := \frac{\alpha}{\bar{h}_{d,r}} |\mathcal{L}_a| m. \quad (28)$$

Using Lemma A.1 and the fact $\alpha_u(r_d^*)$ is increasing in γ_u , we obtain that on the event $\{\tilde{R}_{\mathcal{T}'} = m\}$, the following holds:

$$\alpha_u(r_d^*) \leq \tilde{\alpha}_{a,m} := \frac{1}{\Delta p(1 - \frac{1}{\Delta^2}) + \tilde{\gamma}_{a,m}}. \quad (29)$$

We are now ready to upper bound the right hand side of (24).

Proposition A.2. *Let $a \in \mathcal{B}^*$ and assume that the null p -values are mutually independent, and independent from the non-null p -values. For our testing procedure described in Algorithm 1, the following holds true:*

$$\mathbb{E} \left[\sum_{\mathcal{T}' \in \mathcal{S}(\mathcal{T}_a)} \frac{V_a(\mathcal{T}')}{\tilde{R}_{\mathcal{T}'}} \cdot \mathbb{P}(\mathcal{T}_{a,\text{rej}} = \mathcal{T}' | \mathcal{P}_{\mathcal{T}_a}^c) \right] \leq \alpha \frac{|\mathcal{L}_a|}{p}. \quad (30)$$

The proof of Proposition A.2 uses the equality (26) and the structural properties of the tree \mathcal{T} tree. Its proof is deferred to Section C of the appendix. The bound (23) now follows readily by applying iterative expectation to (30).

Proof of Theorem 3.1. By using the bound (23) and noting that $V = \sum_{a \in \mathcal{B}^*} V_a$, we have

$$\text{FSR} = \sum_{a \in \mathcal{B}^*} \mathbb{E} \left[\frac{V_a}{R \vee 1} \right] = \sum_{a \in \mathcal{B}^*} \mathbb{E} \left[\frac{V_a \mathbb{1}(V_a > 0)}{R} \right] \leq \sum_{a \in \mathcal{B}^*} \frac{|\mathcal{L}_a|}{p} \alpha = \alpha.$$

The result follows. □

A.2 Proof of Theorem 3.2

Theorem 3.2 can be proved by following similar lines of the proof of Theorem 3.1 and so we omit a detailed proof here. The main difference is that in this case, the quantity $\tilde{\alpha}_{a,m}$ should be defined as

$$\tilde{\alpha}_{a,m} := \frac{1}{\Delta p(1 - \frac{1}{\Delta^2}) + \tilde{\gamma}_{a,m}} - \varepsilon_0. \quad (31)$$

Also, the bound (56) is updated as

$$q_{u,m} = \mathbb{P}(u \in \mathcal{T}_{a,\text{rej}}^m) \leq (\tilde{\alpha}_{a,m} + \varepsilon_0)^{\text{depth}(u) - \text{depth}(a) + 1}, \quad (32)$$

and therefore similar to (57) we have

$$\sum_{u \in \mathcal{T}_a} q_{u,m} \leq \frac{1}{\Delta} \cdot \frac{\Delta(\tilde{\alpha}_{a,m} + \varepsilon_0)}{1 - \Delta(\tilde{\alpha}_{a,m} + \varepsilon_0)} = \frac{1}{\Delta p(1 - \frac{1}{\Delta^2})} \tilde{\gamma}_{a,m}, \quad (33)$$

which is the same bound as in (57), albeit via a slightly different derivation and choice of threshold levels $\alpha_u(r)$. The rest of the proof would be identical to the proof of Theorem 3.1.

A.3 Proof of Theorem 3.3

Let $a \in \mathcal{B}^*$, we have

$$\begin{aligned}
\mathbb{E} \left[\frac{V_a}{R} \cdot \mathbb{1}\{V_a > 0\} \right] &= \mathbb{E} \left[\sum_{\mathcal{T}' \in \mathcal{S}(\mathcal{T}_a)} \frac{V_a(\mathcal{T}')}{R} \cdot \mathbb{1}\{\mathcal{T}_{a,\text{rej}} = \mathcal{T}'\} \right] \\
&\leq \left(\Delta - \frac{1}{\Delta}\right) \sum_{\mathcal{T}' \in \mathcal{S}(\mathcal{T}_a)} \mathbb{E} \left[\frac{|\mathcal{T}'|}{R} \cdot \mathbb{1}\{\mathcal{T}_{a,\text{rej}} = \mathcal{T}'\} \right] \\
&= \left(\Delta - \frac{1}{\Delta}\right) \sum_{\mathcal{T}' \in \mathcal{S}(\mathcal{T}_a)} \sum_{u \in \mathcal{T}'} \mathbb{E} \left[\frac{\mathbb{1}\{\mathcal{T}_{a,\text{rej}} = \mathcal{T}'\}}{R} \right] \\
&= \left(\Delta - \frac{1}{\Delta}\right) \sum_{u \in \mathcal{T}_a} \sum_{\mathcal{T}' \in \mathcal{S}(\mathcal{T}_a): u \in \mathcal{T}'} \mathbb{E} \left[\frac{\mathbb{1}\{\mathcal{T}_{a,\text{rej}} = \mathcal{T}'\}}{R} \right] \\
&= \left(\Delta - \frac{1}{\Delta}\right) \sum_{u \in \mathcal{T}_a} \mathbb{E} \left[\frac{\mathbb{1}\{u \in \mathcal{T}_{a,\text{rej}}\}}{R} \right] \\
&= \left(\Delta - \frac{1}{\Delta}\right) \sum_{u \in \mathcal{T}_a} \mathbb{E} \left[\frac{\mathbb{1}\{p_u \leq \alpha_u(r_d^*)\}}{R} \right] \\
&\leq \left(\Delta - \frac{1}{\Delta}\right) \sum_{u \in \mathcal{T}_a} \mathbb{E} \left[\frac{\mathbb{1}\{p_u \leq \alpha_u(r_d^*)\}}{R^{1:(d-1)} + r_d^*} \right] \\
&= \left(\Delta - \frac{1}{\Delta}\right) \sum_{u \in \mathcal{T}_a} \mathbb{E} \left[\frac{\mathbb{1}\left\{p_u \leq \frac{\alpha|\mathcal{L}_u|\beta_d(R^{1:(d-1)} + r_d^*)}{p(\Delta - \frac{1}{\Delta})(D-1)}\right\}}{R^{1:(d-1)} + r_d^*} \right], \tag{34}
\end{aligned}$$

where the first inequality follows from Lemma D.1; the second inequality is because $R \geq R^{1:d} = R^{1:(d-1)} + r_d^*$.

Next, we will use the following proposition by Blanchard & Roquain.

Proposition A.3 (Blanchard & Roquain (2008)). *A couple (U, V) of possibly dependent nonnegative random variables such that U is superuniform, i.e., $\forall t \in [0, 1], \mathbb{P}(U \leq t) \leq t$, satisfy the following inequalities*

$$\forall c > 0, \mathbb{E} \left[\frac{\mathbb{1}\{U \leq c\beta(V)\}}{V} \right] \leq c,$$

if $\beta(\cdot)$ is a shape function of the following form

$$\beta(x) = \int_0^x t d\nu(t),$$

where ν is an arbitrary probability distribution on $(0, \infty)$, and V is arbitrary.

Letting $U = p_u$, $V = R^{1:(d-1)} + r_d^*$, and $c = \frac{\alpha|\mathcal{L}_u|}{p(\Delta - \frac{1}{\Delta})(D-1)}$, we have

$$\begin{aligned} \left(\Delta - \frac{1}{\Delta}\right) \sum_{u \in \mathcal{T}_a} \mathbb{E} \left[\frac{\mathbb{1}\{p_u \leq \alpha_u(r_d^*)\}}{R^{1:(d-1)} + r_d^*} \right] &\leq \left(\Delta - \frac{1}{\Delta}\right) \sum_{u \in \mathcal{T}_a} \frac{\alpha|\mathcal{L}_u|}{p(\Delta - \frac{1}{\Delta})(D-1)} \\ &= \frac{\alpha}{p} \left[\sum_{u \in \mathcal{T}_a} \frac{|\mathcal{L}_u|}{D-1} \right] \\ &\leq \frac{\alpha|\mathcal{L}_a|}{p}, \end{aligned}$$

where the last inequality follows from

$$\sum_{u \in \mathcal{T}_a} |\mathcal{L}_u| \leq \sum_{d=2}^D \sum_{u \in \mathcal{T}^d \cap \mathcal{T}_a} |\mathcal{L}_u| = \sum_{d=2}^D |\mathcal{L}_a| = (D-1)|\mathcal{L}_a|.$$

It is reasonable to use a measure ν that puts mass proportional to $\frac{1}{x}$ only on the values that its arguments could possibly take. By the design of the tree, we have

$$R^{1:(d-1)} + r_d^* \geq (d-1)(\delta-1) + \delta - 1 = d(\delta-1),$$

since at least one node has to be rejected on each depth from 1 to $d-1$ for the algorithm to carry on to depth d , and

$$R^{1:(d-1)} + r_d^* \leq \sum_{u \in \mathcal{T}^{d-1}} \deg_{\mathcal{T}}(u) - 1.$$

Therefore,

$$\beta_d(R^{1:(d-1)} + r_d^*) = \frac{R^{1:(d-1)} + r_d^*}{\sum_{k=d(\delta-1)}^{\sum_{u \in \mathcal{T}^{d-1}} \deg_{\mathcal{T}}(u) - 1} \frac{1}{k}}.$$

The rest of the proof is identical to the proof of Theorem 3.1.

A.3.1 Proof of Theorem 3.4

The result of theorem can be derived by a similar argument used in the proof of Theorem 3.3. We leave out a detailed proof and only highlight the required modifications to the proof of Theorem 3.3.

Following the chain of inequalities in (34) we have that for $a \in \mathcal{B}^*$,

$$\begin{aligned}
\mathbb{E} \left[\frac{V_a}{R} \cdot \mathbb{1}\{V_a > 0\} \right] &\leq \left(\Delta - \frac{1}{\Delta}\right) \sum_{u \in \mathcal{T}_a} \mathbb{E} \left[\frac{\mathbb{1}\{p_u \leq \alpha_u(r_d^*)\}}{R^{1:(d-1)} + r_d^*} \right] \\
&= \left(\Delta - \frac{1}{\Delta}\right) \sum_{u \in \mathcal{T}_a} \mathbb{E} \left[\frac{\mathbb{1}\left\{p_u \leq \frac{\alpha|\mathcal{L}_u|\beta_d(R^{1:(d-1)}+r_d^*)}{p(\Delta-\frac{1}{\Delta})(D-1)} - \varepsilon_0\right\}}{R^{1:(d-1)} + r_d^*} \right] \\
&= \left(\Delta - \frac{1}{\Delta}\right) \sum_{u \in \mathcal{T}_a} \mathbb{E} \left[\frac{\mathbb{1}\left\{p_u + \varepsilon_0 \leq \frac{\alpha|\mathcal{L}_u|\beta_d(R^{1:(d-1)}+r_d^*)}{p(\Delta-\frac{1}{\Delta})(D-1)} - \varepsilon_0\right\}}{R^{1:(d-1)} + r_d^*} \right] \tag{35}
\end{aligned}$$

where we used the definition of threshold function $\alpha_u(r_d^*)$ given by (14). Also by theorem assumption $p_u + \varepsilon_0$ is super-uniform because

$$\mathbb{P}(p_u + \varepsilon_0 \leq t) = \mathbb{P}(p_u \leq t - \varepsilon_0) \leq (t - \varepsilon_0) + \varepsilon_0 = t.$$

Therefore we can apply Proposition A.3 with $U = p_u + \varepsilon_0$, $V = R^{1:(d-1)} + r_d^*$, and $c = \frac{\alpha|\mathcal{L}_u|}{p(\Delta-\frac{1}{\Delta})(D-1)}$. The rest of the proof is identical to the proof of Theorem 3.3 and is omitted.

B Proof of technical lemmas

B.1 Proof of Lemma 2.1

Following the example given in Figure 1, we use solid shape for true barriers and dashed shape for achieved barriers. Therefore, FDP^b can be written as

$$\text{FDP}^b = \frac{|i \in [p-1] : \vartheta_i^* = 0, \widehat{\vartheta}_i = 1|}{|i \in [p-1] : \widehat{\vartheta}_i = 1|} = \frac{\#\{\text{slots with dashed but not solid barriers}\}}{\#\{\text{slots with dashed barriers}\}}.$$

Similarly, we can write TPP^b as

$$\text{TPP}^b = \frac{|i \in [p-1] : \vartheta_i^* = 1, \widehat{\vartheta}_i = 1|}{|i \in [p-1] : \vartheta_i^* = 1|} = \frac{\#\{\text{slots with solid and dashed barriers}\}}{\#\{\text{slots with solid barriers}\}},$$

where $(\mathcal{R}^b)^C := (\mathcal{H}_0^b \cup \mathcal{H}_1^b) \setminus \mathcal{R}^b$ is the set of non-rejections.

Furthermore, we know that n barriers yield $(n + 1)$ groups. Hence

$$\#\{\text{slots with only dashed barriers}\} = M - 1$$

and

$$\#\{\text{slots with only solid barriers}\} = K - 1.$$

Fixing the solid barriers, any dashed barrier in a slot where a solid barrier does not already exist will divide one true group into two. That is to say, within each true group C_i^* , the number of dashed barriers, say m , will yield $(m+1)$ pairs of $\{i, j\}$ such that $C_i^* \cap \widehat{C}_j \neq \emptyset$. Therefore,

$$\begin{aligned} \#\{\text{slots with dashed but not solid barriers}\} &= \sum_{i=1}^K \left(\sum_{j=1}^M \mathbb{1}\{C_i^* \cap \widehat{C}_j \neq \emptyset\} - 1 \right) \\ &= \sum_{i=1}^K \left(\sum_{j=1}^M \mathbb{1}\{C_i^* \cap \widehat{C}_j \neq \emptyset\} \right) - K. \end{aligned}$$

Similarly, by exchanging the role of dashed and solid barriers, we also get

$$\begin{aligned} \#\{\text{slots with solid but not dashed barriers}\} &= \sum_{i=1}^M \left(\sum_{j=1}^K \mathbb{1}\{C_i^* \cap \widehat{C}_j \neq \emptyset\} - 1 \right) \\ &= \sum_{i=1}^M \left(\sum_{j=1}^K \mathbb{1}\{C_i^* \cap \widehat{C}_j \neq \emptyset\} \right) - M. \end{aligned}$$

Finally, by plugging in the terms, we can draw the equivalence between FDP^b and FSP, as well as the two true positive proportions.

B.2 Proof of Lemma 2.2

We will prove the lemma by showing that

$$\max \left\{ \sum_{u \in \mathcal{T}_{\text{rej}}} (\deg_{\mathcal{T}}(u) - \deg_{\mathcal{T}_{\text{rej}}}(u)) - 1, 0 \right\} = M - 1. \quad (36)$$

and

$$\sum_{u \in \mathcal{F}} (\deg_{\mathcal{T}}(u) - \deg_{\mathcal{T}_{\text{rej}}}(u)) - |\mathcal{B}^* \cap \mathcal{F}| = \sum_{i=1}^K \left(\sum_{j=1}^M \mathbb{1}\{C_i^* \cap \widehat{C}_j \neq \emptyset\} \right) - K, \quad (37)$$

The proof is based on induction on the depth of the tree D .

We first prove the induction basis when $D = 2$. In this case, \mathcal{T} consists in one root node u_0 and its children as leaves. We therefore have only one hypothesis, $\mathcal{H}_{u_0}^0$.

- If $\mathcal{H}_{u_0}^0$ fails to be rejected, then $\mathcal{F} = \mathcal{T}_{\text{rej}} = \emptyset$, $M = 1$. Both left hand side and right hand side of equation (36) are 0. For equation (37), the left hand side is clearly 0, and the right hand side is also 0 since $\sum_{i=1}^K \left(\sum_{j=1}^M \mathbb{1}\{C_i^* \cap \widehat{C}_j \neq \emptyset\} \right) - K = (\sum_{i=1}^K 1) - K = 0$.
- If $\mathcal{H}_{u_0}^0$ is rejected, we will have $M = \deg_{\mathcal{T}}(u_0)$ and $\mathcal{T}_{\text{rej}} = \{u_0\}$. Equation (36) holds because $\sum_{u \in \mathcal{T}_{\text{rej}}} (\deg_{\mathcal{T}}(u) - \deg_{\mathcal{T}_{\text{rej}}}(u)) - 1 = \deg_{\mathcal{T}}(u_0) - \deg_{\mathcal{T}_{\text{rej}}}(u_0) - 1 = M - 1$ since $\deg_{\mathcal{T}_{\text{rej}}}(u_0) = 0$. For equation (37), we consider two scenarios:

- If $\mathcal{H}_{u_0}^0$ is true, then $K = |\mathcal{B}^*| = 1$ and $\mathcal{F} = \mathcal{T}_{\text{rej}} = \{u_0\}$. So the left hand side of (37) becomes $\deg_{\mathcal{T}}(u_0) - 1 = M - 1$, and the right hand side becomes $M - K = M - 1$, hence the equality holds.
- Otherwise $\mathcal{H}_{u_0}^0$ is false and $K = |\mathcal{B}^*| = \deg_{\mathcal{T}}(u_0) = M$, and $\mathcal{F} = \emptyset$. So the left hand side of (37) becomes 0, and the right hand side becomes $M - K = 0$, hence the equality holds.

Next we proceed by proving the induction step for equation (36). Let $D > 2$ be an arbitrary integer. We assume for a tree with maximum depth $\leq D - 1$, identity (36) holds. We want to show that it holds for a tree with maximum depth D .

Clearly, this equation holds when the root node is not rejected, i.e., $\mathcal{T}_{\text{rej}} = \emptyset$ and $M = 1$. We henceforth discuss the case that the root node is rejected. In this case, equation (36) can be simplified as

$$\sum_{u \in \mathcal{T}_{\text{rej}}} (\deg_{\mathcal{T}}(u) - \deg_{\mathcal{T}_{\text{rej}}}(u)) = M.$$

For a tree \mathcal{T} with maximum depth D , if we remove the root node, we will be left with a forest where each tree is of maximum depth less than D . Within each tree, we have that identity (36) holds by the induction hypothesis. We refer to the set of trees in the forest as S_{root} . Furthermore, we use $M_{\mathcal{T}'}, \mathcal{T}' \in S_{\text{root}}$ for the number of achieved groups in each such tree. Obviously,

$$\sum_{\mathcal{T}' \in S_{\text{root}}} M_{\mathcal{T}'} = M. \quad (38)$$

Therefore,

$$\begin{aligned} & \sum_{u \in \mathcal{T}_{\text{rej}}} (\deg_{\mathcal{T}}(u) - \deg_{\mathcal{T}_{\text{rej}}}(u)) \\ &= \sum_{u \in \mathcal{T}_{\text{rej}} \setminus \{\text{root}\}} (\deg_{\mathcal{T}}(u) - \deg_{\mathcal{T}_{\text{rej}}}(u)) + \deg_{\mathcal{T}}(\text{root}) - \deg_{\mathcal{T}_{\text{rej}}}(\text{root}) \\ &= \sum_{\mathcal{T}' \in S_{\text{root}}} \sum_{u \in \mathcal{T}_{\text{rej}} \cap \mathcal{T}'} (\deg_{\mathcal{T}}(u) - \deg_{\mathcal{T}_{\text{rej}}}(u)) + \deg_{\mathcal{T}}(\text{root}) - \deg_{\mathcal{T}_{\text{rej}}}(\text{root}) \\ &= \sum_{\substack{\mathcal{T}' \in S_{\text{root}} \\ \mathcal{T}' \cap \mathcal{T}_{\text{rej}} \neq \emptyset}} \sum_{u \in \mathcal{T}_{\text{rej}} \cap \mathcal{T}'} (\deg_{\mathcal{T}}(u) - \deg_{\mathcal{T}_{\text{rej}}}(u)) + \deg_{\mathcal{T}}(\text{root}) - \deg_{\mathcal{T}_{\text{rej}}}(\text{root}) \\ &= \sum_{\substack{\mathcal{T}' \in S_{\text{root}} \\ \mathcal{T}' \cap \mathcal{T}_{\text{rej}} \neq \emptyset}} M_{\mathcal{T}'} + \deg_{\mathcal{T}}(\text{root}) - \deg_{\mathcal{T}_{\text{rej}}}(\text{root}) \\ &= \sum_{\substack{\mathcal{T}' \in S_{\text{root}} \\ \mathcal{T}' \cap \mathcal{T}_{\text{rej}} \neq \emptyset}} M_{\mathcal{T}'} + \sum_{\substack{\mathcal{T}' \in S_{\text{root}} \\ \mathcal{T}' \cap \mathcal{T}_{\text{rej}} = \emptyset}} M_{\mathcal{T}'} \\ &= M, \end{aligned}$$

where the fourth equality is by the induction hypothesis; the fifth equality holds because there are $\deg_{\mathcal{T}}(\text{root}) - \deg_{\mathcal{T}_{\text{rej}}}(\text{root})$ subtrees $\mathcal{T}' \in S_{\text{root}}$ such that $\mathcal{T}' \cap \mathcal{T}_{\text{rej}} = \emptyset$, and their $M_{\mathcal{T}'} = 1$; the last equality follows from (38). This proves the induction step and hence completes the proof of identity (36).

We next proceed to prove (37). Suppose that the induction hypothesis holds for trees with depth at most $D - 1$. We want to prove it for trees of depth D . Note that this identity trivially holds when the root is not rejected, and therefore we focus on the case where the root is rejected. There are two scenarios: (1) the root is a true rejection, or (2) the root is a false rejection.

We first assume the root is a true rejection. Then we have

$$K = \sum_{\mathcal{T}' \in S_{\text{root}}} K_{\mathcal{T}'}, \quad (39)$$

where $K_{\mathcal{T}'} \geq 1$ is defined as the number of true groups in each $\mathcal{T}' \in S_{\text{root}}$.

Then the left hand side of (37) becomes

$$\begin{aligned} & \sum_{u \in \mathcal{F}} \left(\deg_{\mathcal{T}}(u) - \deg_{\mathcal{T}_{\text{rej}}}(u) \right) - |\mathcal{B}^* \cap \mathcal{F}| \\ &= \sum_{\mathcal{T}' \in S_{\text{root}}} \left(\sum_{u \in \mathcal{F} \cap \mathcal{T}'} \deg_{\mathcal{T}}(u) - \deg_{\mathcal{T}_{\text{rej}}}(u) - |\mathcal{B}^* \cap \mathcal{F} \cap \mathcal{T}'| \right) \\ &= \sum_{\mathcal{T}' \in S_{\text{root}}} \left[\sum_{1 \leq i \leq K_{\mathcal{T}'}} \left(\sum_{1 \leq j \leq M_{\mathcal{T}'}} \mathbb{1}\{C_i^* \cap \hat{C}_j \neq \emptyset\} \right) - K_{\mathcal{T}'} \right] \\ &= \sum_{1 \leq i \leq K} \left(\sum_{1 \leq j \leq M} \mathbb{1}\{C_i^* \cap \hat{C}_j \neq \emptyset\} \right) - K, \end{aligned}$$

where the first equality holds because $\mathcal{T}' \in S_{\text{root}}$ are disjoint from each other and the root is not in $\mathcal{B}^* \cap \mathcal{F}$; the second equality follows from the induction hypothesis, and the last equality follows from (38) and (39).

For the case where the root is a false rejection, we have $K = 1$, $\mathcal{B}^* = \{\text{root}\}$ and any rejection is a false rejection ($\mathcal{F} = \mathcal{T}_{\text{rej}}$). We write

$$\sum_{u \in \mathcal{F}} \left(\deg_{\mathcal{T}}(u) - \deg_{\mathcal{T}_{\text{rej}}}(u) \right) - |\mathcal{B}^* \cap \mathcal{F}| = \sum_{u \in \mathcal{T}_{\text{rej}}} \left(\deg_{\mathcal{T}}(u) - \deg_{\mathcal{T}_{\text{rej}}}(u) \right) - 1 = M - 1,$$

where in the last step we used identity (36). On the other hand, in this case there is only one true group ($K = 1$) which consists of all leaves. Therefore, any returned group \hat{C}_j will intersect with it and we get

$$\sum_{i=1}^K \left(\sum_{j=1}^M \mathbb{1}\{C_i^* \cap \hat{C}_j \neq \emptyset\} \right) - 1 = M - 1.$$

Comparing the previous two equations implies that identity (37) holds for the tree \mathcal{T} . This completes the induction step and hence proves identity (37).

B.3 Proof of Lemma 2.3

The proof of Lemma 2.3 follows from Lemma 2.2 and that $\deg_{\mathcal{T}}(u) = 2$, for all non-leaf nodes $u \in \mathcal{T}$. It suffices to show

$$\sum_{u \in \mathcal{F}} \left(\deg_{\mathcal{T}}(u) - \deg_{\mathcal{T}_{\text{rej}}}(u) \right) - |\mathcal{B}^* \cap \mathcal{F}| = |\mathcal{F}|, \quad (40)$$

and

$$\max \left\{ \sum_{u \in \mathcal{T}_{\text{rej}}} (\deg_{\mathcal{T}}(u) - \deg_{\mathcal{T}_{\text{rej}}}(u)) - 1, 0 \right\} = |\mathcal{T}_{\text{rej}}|. \quad (41)$$

To prove equation (40), note that if a node is falsely rejected all of its rejected children are also false rejections. Therefore, $\sum_{u \in \mathcal{F}} \deg_{\mathcal{T}_{\text{rej}}}(u)$ counts the total number of edges where both nodes of it are in \mathcal{F} . Hence,

$$\begin{aligned} & \sum_{u \in \mathcal{F}} \left(\deg_{\mathcal{T}}(u) - \deg_{\mathcal{T}_{\text{rej}}}(u) \right) - |\mathcal{B}^* \cap \mathcal{F}| \\ &= 2|\mathcal{F}| - |\{u : u \in \mathcal{F}, \text{parent}(u) \in \mathcal{F}\}| - |\mathcal{B}^* \cap \mathcal{F}| \\ &= 2|\mathcal{F}| - |\{u : u \in \mathcal{F}, \text{parent}(u) \in \mathcal{F}\}| - |\{u : u \in \mathcal{F}, \text{parent}(u) \notin \mathcal{F}\}| \\ &= 2|\mathcal{F}| - |\mathcal{F}| \\ &= |\mathcal{F}|. \end{aligned}$$

Equation (41) holds trivially when $|\mathcal{T}_{\text{rej}}| = 0$. When $|\mathcal{T}_{\text{rej}}| > 0$, the root node is rejected, and we write

$$\begin{aligned} & \sum_{u \in \mathcal{T}_{\text{rej}}} (\deg_{\mathcal{T}}(u) - \deg_{\mathcal{T}_{\text{rej}}}(u)) - 1 \\ &= 2|\mathcal{T}_{\text{rej}}| - \sum_{u \in \mathcal{T}_{\text{rej}}} \deg_{\mathcal{T}_{\text{rej}}}(u) - 1 \\ &= 2|\mathcal{T}_{\text{rej}}| - (|\mathcal{T}_{\text{rej}}| - 1) - 1 \\ &= |\mathcal{T}_{\text{rej}}|. \end{aligned}$$

This completes the proof.

B.4 Proof of Lemma 4.1

We use the shorthand $\ell_u := |\mathcal{L}_u|$ for a node u . Define the random vector $\mathbf{w} \in \mathbb{R}^{\Delta_a}$ with elements $w_u = \ell_u^{1/2} \bar{y}_u$ and the fixed unit vector $\mathbf{r} \in \mathbb{R}^{\Delta_a}$ with elements $r_u = (\ell_u/\ell_a)^{1/2}$. We have

$$\mathbf{r}^\top \mathbf{w} = \sum_{u \in \text{child}(a)} (\ell_u/\ell_a)^{1/2} (\ell_u^{1/2} \bar{y}_u) = \ell_a^{-1/2} \sum_{u \in \text{child}(a)} \ell_u \bar{y}_u = \ell_a^{1/2} \bar{y}_a, \quad (42)$$

from which it follows that

$$\sum_{u \in \text{child}(a)} \ell_u (\bar{y}_u - \bar{y}_a)^2 = \sum_{u \in \text{child}(a)} (\ell_u^{1/2} (\bar{y}_u - \bar{y}_a))^2 = \sum_{u \in \text{child}(a)} (w_u - r_u \mathbf{r}^\top \mathbf{w})^2 = \|(\mathbf{I}_{\Delta_a} - \mathbf{r} \mathbf{r}^\top) \mathbf{w}\|^2.$$

The random vector \mathbf{w} is multivariate normal with $\mathbb{E}[w_u] = \ell_u^{1/2} \bar{\theta}_u$, where $\bar{\theta}_u = \frac{1}{|\mathcal{L}_u|} \sum_{i \in \mathcal{L}_u} \theta_i$ is the average of parameters on the leaf nodes \mathcal{L}_u . In addition, $\text{Cov}(\mathbf{w}) = \sigma^2 \mathbf{I}_{\Delta_a}$. Taking the expectation of (42) establishes that

$$\mathbb{E}[(\mathbf{r} \mathbf{r}^\top \mathbf{w})_u] = \mathbb{E}[r_u (\mathbf{r}^\top \mathbf{w})] = (\ell_u / \ell_a)^{1/2} \ell_a^{1/2} \mathbb{E}[\bar{y}_a] = \ell_u^{1/2} \bar{\theta}_a.$$

Under \mathcal{H}_a , we have $\bar{\theta}_u = \bar{\theta}_a$ and thus

$$(\mathbf{I}_{\Delta_a} - \mathbf{r} \mathbf{r}^\top) \mathbf{w} \sim \mathbf{N}(\mathbf{0}, \sigma^2 (\mathbf{I}_{\Delta_a} - \mathbf{r} \mathbf{r}^\top)),$$

where we use the fact that $\|\mathbf{r}\|_2 = 1$ and so $\mathbf{I}_{\Delta_a} - \mathbf{r} \mathbf{r}^\top$ is a projection matrix. This establishes that

$$\sum_{u \in \text{child}(a)} \ell_u (\bar{y}_u - \bar{y}_a)^2 \sim \sigma^2 \chi_{\Delta_a - 1}^2$$

under \mathcal{H}_a , meaning that p_a is uniform. Now consider some node $b \neq a$. If $\mathcal{L}_a \cap \mathcal{L}_b = \emptyset$, then p_a and p_b are clearly independent (because they depend only on $\mathbf{y}_{\mathcal{L}_a}$ and $\mathbf{y}_{\mathcal{L}_b}$, respectively). Thus, it remains to consider the case that $\mathcal{L}_a \subset \mathcal{L}_b$ (i.e., a is a descendant of b). There must exist $v \in \text{child}(b)$ with $\mathcal{L}_a \subseteq \mathcal{L}_v \subset \mathcal{L}_b$. From (15), $p_b = f(\bar{y}_v, \mathbf{y}_{\mathcal{L}_b \setminus \mathcal{L}_v})$. Since $(\mathcal{L}_b \setminus \mathcal{L}_v) \cap \mathcal{L}_a = \emptyset$, we know that p_a is independent of $\mathbf{y}_{\mathcal{L}_b \setminus \mathcal{L}_v}$. It therefore remains to show that p_a is also independent of \bar{y}_v . To do so, observe that

$$\ell_v \bar{y}_v = \sum_{i \in \mathcal{L}_a} y_i + \sum_{i \in \mathcal{L}_v \setminus \mathcal{L}_a} y_i = \ell_a^{1/2} \mathbf{r}^\top \mathbf{w} + \sum_{i \in \mathcal{L}_v \setminus \mathcal{L}_a} y_i. \quad (43)$$

Thus,

$$\begin{aligned} \text{Cov}([\mathbf{I}_{\Delta_a} - \mathbf{r} \mathbf{r}^\top] \mathbf{w}, \bar{y}_v) &= \ell_v^{-1} \text{Cov}([\mathbf{I}_{\Delta_a} - \mathbf{r} \mathbf{r}^\top] \mathbf{w}, \ell_v \bar{y}_v) \\ &= \ell_a^{1/2} \ell_v^{-1} \text{Cov}([\mathbf{I}_{\Delta_a} - \mathbf{r} \mathbf{r}^\top] \mathbf{w}, \mathbf{r}^\top \mathbf{w}) \\ &= \sigma^2 \ell_a^{1/2} \ell_v^{-1} [\mathbf{I}_{\Delta_a} - \mathbf{r} \mathbf{r}^\top] \mathbf{r} \\ &= 0, \end{aligned}$$

where the first equality follows from observing that the second term in (43) is independent of \mathbf{w} (which depends only on $\mathbf{y}_{\mathcal{L}_a}$) and the second inequality uses that $\text{Cov}(\mathbf{w}) = \sigma^2 \mathbf{I}_{\Delta_a}$. This establishes that p_a is independent of p_b .

B.5 Proof of Proposition 4.2

Note that for any node u , we have $\|\mathbf{G}_u\|_2 = 1$ since \mathbf{G}_u is a projection matrix. Also, by using (Guo et al. 2019, Lemma 2) (which itself follows from (Cai et al. 2019a, Lemma 1)), we have

$$\|\mathbf{G}_u \hat{\boldsymbol{\theta}}\|_2 \leq c_0 (\hat{\mathbf{b}}^\top \hat{\boldsymbol{\Sigma}} \hat{\mathbf{b}})^{1/2}, \quad (44)$$

for some constant $c_0 > 0$. This inequality follows by analyzing the optimization (17) which is used to define the direction $\widehat{\mathbf{b}}$. Therefore, for any node u , we obtain

$$\begin{aligned}
\frac{\|\mathbf{G}_u \widehat{\boldsymbol{\theta}}\|_2 + \|\mathbf{G}_u\|_2}{\sqrt{\widehat{\text{Var}}_\tau(\widehat{Q}_u^d)} &\leq \frac{c_0(\widehat{\mathbf{b}}^\top \widehat{\boldsymbol{\Sigma}} \widehat{\mathbf{b}})^{1/2} + 1}{\sqrt{\widehat{\text{Var}}_\tau(\widehat{Q}_u^d)}} \\
&= \frac{c_0(\widehat{\mathbf{b}}^\top \widehat{\boldsymbol{\Sigma}} \widehat{\mathbf{b}})^{1/2} + 1}{\sqrt{\frac{4\widehat{\sigma}^2}{n} \widehat{\mathbf{b}}^\top \widehat{\boldsymbol{\Sigma}} \widehat{\mathbf{b}} + \frac{\tau}{n}}} \\
&\leq \frac{c_0 \sqrt{n}}{2\widehat{\sigma}} + \sqrt{\frac{n}{\tau}}.
\end{aligned} \tag{45}$$

Define $x := \Phi^{-1}(1 - \frac{t}{2})$ and

$$\eta_n := c_1 \left(\frac{c_0}{2\widehat{\sigma}} + \sqrt{\frac{1}{\tau}} \right) \frac{s_0 \log p}{\sqrt{n}}, \tag{46}$$

with c_1 given in (19). Under the null hypothesis $\widetilde{\mathcal{H}}_{0,u}$ (or equivalently $\mathcal{H}_{0,u}$), we have for all $t \in [0, 1]$,

$$\begin{aligned}
\mathbb{P}(p_u \leq t) &= \mathbb{P} \left(\Phi^{-1}(1 - \frac{t}{2}) \leq \frac{|\widehat{Q}_u^d|}{\sqrt{\widehat{\text{Var}}_\tau(\widehat{Q}_u)}} \right) \\
&= \mathbb{P} \left(x \leq \frac{|\widehat{Q}_u^d|}{\sqrt{\widehat{\text{Var}}_\tau(\widehat{Q}_u)}} \right) \\
&= \mathbb{P} \left(x \leq \frac{|Z_u + \Delta_u|}{\sqrt{\widehat{\text{Var}}_\tau(\widehat{Q}_u)}} \right) \\
&\leq \mathbb{P} \left(x - \eta_n \leq \frac{|Z_u|}{\sqrt{\widehat{\text{Var}}_\tau(\widehat{Q}_u)}} \right) + \mathbb{P} \left(\eta_n \leq \frac{|\Delta_u|}{\sqrt{\widehat{\text{Var}}_\tau(\widehat{Q}_u)}} \right).
\end{aligned} \tag{47}$$

By using the bias bound (19), together with (45) and definition of η_n given by (46), we have

$$\mathbb{P} \left(\eta_n \leq \frac{|\Delta_u|}{\sqrt{\widehat{\text{Var}}_\tau(\widehat{Q}_u)}} \right) \leq 2pe^{-c_2 n}, \tag{48}$$

for all nodes u . In addition,

$$\begin{aligned}
& \mathbb{P} \left(x - \eta_n \leq \frac{|Z_u|}{\sqrt{\widehat{\text{Var}}_\tau(\widehat{Q}_u)}} \right) \\
& \leq \mathbb{P} \left(x - \eta_n \leq \frac{|Z_u|}{\sqrt{\frac{4\widehat{\sigma}^2}{n} \widehat{\mathbf{b}}^\top \widehat{\Sigma} \widehat{\mathbf{b}}}} \right) = \mathbb{P} \left(x - \eta_n \leq \frac{\sigma|Z_u|}{\widehat{\sigma} \sqrt{\text{Var}(\widehat{Q}_u^d)}} \right) \\
& \leq \mathbb{P} \left((x - \eta_n)(1 - \varepsilon) \leq \frac{|Z_u|}{\sqrt{\text{Var}(\widehat{Q}_u^d)}} \right) + \mathbb{P} \left(\left| \frac{\widehat{\sigma}}{\sigma} - 1 \right| \geq \varepsilon \right) \\
& = 2\Phi(\varepsilon x - x + \eta_n - \varepsilon \eta_n) + \mathbb{P} \left(\left| \frac{\widehat{\sigma}}{\sigma} - 1 \right| \geq \varepsilon \right) \tag{49}
\end{aligned}$$

Combining (47), (48) and (49) we obtain

$$\mathbb{P}(p_u \leq t) \leq 2\Phi(\varepsilon x - x + \eta_n - \varepsilon \eta_n) + \mathbb{P} \left(\left| \frac{\widehat{\sigma}}{\sigma} - 1 \right| \geq \varepsilon \right) + 2pe^{-c_2 n}.$$

Note that the right-hand side of the above equation does not depend on the node u . In other words, it is a uniform bound for all nodes. Under the condition $s_0(\log p)/\sqrt{n} \rightarrow 0$, we have $\eta_n \rightarrow 0$ as $n \rightarrow \infty$. Therefore, for any fixed $\varepsilon_0 > 0$, by choosing $\varepsilon > 0$ small enough and $n_0 = n_0(\varepsilon)$ large enough we can ensure that for all $n \geq n_0$

$$\mathbb{P}(p_u \leq t) \leq 2\Phi(-x) + \varepsilon_0 = 2(1 - \Phi(x)) + \varepsilon_0 = t + \varepsilon_0,$$

for all nodes u .

C Proof of Proposition A.2

For depth d we define the quantities $L_d := R^{1:(d-1)} + r_d^*$ and $U_d := p-1 - (\sum_{u \in \mathcal{T}^d} \deg_{\mathcal{T}}(u) - |\mathcal{T}^d| - r_d^*)$. For node $a \in \mathcal{B}^*$ with $\text{depth}(a) = d$, we write

$$\begin{aligned}
& \sum_{\mathcal{T}' \in S(\mathcal{T}_a)} \frac{V_a(\mathcal{T}')}{\tilde{R}_{\mathcal{T}'}} \cdot \mathbb{P}(\mathcal{T}_{a,\text{rej}} = \mathcal{T}' | \mathcal{P}_{\mathcal{T}_a}^c) \\
& \stackrel{(a)}{\leq} \left(\Delta - \frac{1}{\Delta}\right) \sum_{\mathcal{T}' \in S(\mathcal{T}_a)} \frac{|\mathcal{T}'|}{\tilde{R}_{\mathcal{T}'}} \mathbb{P}(\mathcal{T}_{a,\text{rej}} = \mathcal{T}' | \mathcal{P}_{\mathcal{T}_a}^c) \\
& = \left(\Delta - \frac{1}{\Delta}\right) \sum_{\mathcal{T}' \in S(\mathcal{T}_a)} \sum_{u \in \mathcal{T}'} \frac{1}{\tilde{R}_{\mathcal{T}'}} \mathbb{P}(\mathcal{T}_{a,\text{rej}} = \mathcal{T}' | \mathcal{P}_{\mathcal{T}_a}^c) \\
& = \left(\Delta - \frac{1}{\Delta}\right) \sum_{u \in \mathcal{T}_a} \sum_{\mathcal{T}' \in S(\mathcal{T}_a): u \in \mathcal{T}'} \frac{1}{\tilde{R}_{\mathcal{T}'}} \mathbb{P}(\mathcal{T}_{a,\text{rej}} = \mathcal{T}' | \mathcal{P}_{\mathcal{T}_a}^c) \\
& \stackrel{(b)}{\leq} \left(\Delta - \frac{1}{\Delta}\right) \sum_{u \in \mathcal{T}_a} \sum_{m=L_d}^{U_d} \sum_{\mathcal{T}' \in S(\mathcal{T}_a): u \in \mathcal{T}'} \frac{1}{\tilde{R}_{\mathcal{T}'}} \mathbb{P}(\mathcal{T}_{a,\text{rej}} = \mathcal{T}' | \mathcal{P}_{\mathcal{T}_a}^c) \mathbb{1}(\tilde{R}_{\mathcal{T}'} = m) \\
& = \left(\Delta - \frac{1}{\Delta}\right) \sum_{u \in \mathcal{T}_a} \sum_{m=L_d}^{U_d} \frac{1}{m} \sum_{\mathcal{T}' \in S(\mathcal{T}_a)} \mathbb{P}(\mathcal{T}_{a,\text{rej}} = \mathcal{T}' | \mathcal{P}_{\mathcal{T}_a}^c) \mathbb{1}(\tilde{R}_{\mathcal{T}'} = m, u \in \mathcal{T}') \\
& = \left(\Delta - \frac{1}{\Delta}\right) \sum_{u \in \mathcal{T}_a} \sum_{m=L_d}^{U_d} \frac{1}{m} \mathbb{P}(\tilde{R}_{\mathcal{T}_{a,\text{rej}}} = m, u \in \mathcal{T}_{a,\text{rej}} | \mathcal{P}_{\mathcal{T}_a}^c). \tag{50}
\end{aligned}$$

Here (a) follows from Lemma D.2, and (b) holds since for $\mathcal{T}' \in S(\mathcal{T}_a)$, the number of total rejections $\tilde{R}_{\mathcal{T}'}$ satisfies

$$L_d \leq \tilde{R}_{\mathcal{T}'} \leq U_d.$$

The lower bound holds trivially since $\mathcal{T}' \in S(\mathcal{T}_a)$ and $\text{depth}(a) = d$. The number of splits made by algorithm up to level d is $R^{1:d} = R^{1:(d-1)} + r_d^*$ by using Equation (25). For the upper bound, note that one can split the p leaves at most $p-1$ times. Now focusing on nodes in depth d , rejecting a node u results in $\deg_{\mathcal{T}}(u) - 1$ additional splits. So the nodes in depth d can make up to $\sum_{u \in \mathcal{T}^d} \deg_{\mathcal{T}}(u) - |\mathcal{T}^d|$ additional splits, while the algorithm makes r_d^* additional splits as we discussed in Equation (25). So the difference between these two quantities, $\sum_{u \in \mathcal{T}^d} \deg_{\mathcal{T}}(u) - |\mathcal{T}^d| - r_d^*$, is the number of potential splits that the testing rule has missed while testing nodes at depth d . This argument implies that the total number of splits can go up to $U_d = p-1 - (\sum_{u \in \mathcal{T}^d} \deg_{\mathcal{T}}(u) - |\mathcal{T}^d| - r_d^*)$.

Now by using bound (29), on the event $\{\tilde{R}_{\mathcal{T}'} = m\}$ we have $\alpha_u(r_d^*) \leq \tilde{\alpha}_{a,m}$. Define $\mathcal{T}_{a,\text{rej}}^m$ as the rejection subtree as if the test levels $\alpha_u(r_d^*)$ are replaced by $\tilde{\alpha}_{a,m}$. Therefore $\mathcal{T}_{a,\text{rej}} \subseteq \mathcal{T}_{a,\text{rej}}^m$, which implies

$$\mathbb{P}(\tilde{R}_{\mathcal{T}_{a,\text{rej}}} = m, u \in \mathcal{T}_{a,\text{rej}} | \mathcal{P}_{\mathcal{T}_a}^c) \leq \mathbb{P}(\tilde{R}_{\mathcal{T}_{a,\text{rej}}^m} = m, u \in \mathcal{T}_{a,\text{rej}}^m | \mathcal{P}_{\mathcal{T}_a}^c).$$

Combining this inequality with (50) and taking the expectation gives

$$\mathbb{E} \left[\sum_{\mathcal{T}' \in \mathcal{S}(\mathcal{T}_a)} \frac{V_a(\mathcal{T}')}{\tilde{R}_{\mathcal{T}'}} \cdot \mathbb{P}(\mathcal{T}_{a,\text{rej}} = \mathcal{T}' | \mathcal{P}_{\mathcal{T}_a}^c) \right] \leq (\Delta - \frac{1}{\Delta}) \sum_{u \in \mathcal{T}_a} \sum_{m=L_d}^{U_d} \frac{1}{m} \mathbb{P}(\tilde{R}_{\mathcal{T}_{a,\text{rej}}} = m, u \in \mathcal{T}_{a,\text{rej}}^m). \quad (51)$$

Focusing on the innermost summation, we have

$$\begin{aligned} & \sum_{m=L_d}^{U_d} \frac{1}{m} \mathbb{P}(\tilde{R}_{\mathcal{T}_{a,\text{rej}}} = m, u \in \mathcal{T}_{a,\text{rej}}^m) \\ &= \sum_{m=L_d}^{U_d} \frac{1}{m} \left[\mathbb{P}(\tilde{R}_{\mathcal{T}_{a,\text{rej}}} \geq m, u \in \mathcal{T}_{a,\text{rej}}^m) - \mathbb{P}(\tilde{R}_{\mathcal{T}_{a,\text{rej}}} \geq m+1, u \in \mathcal{T}_{a,\text{rej}}^m) \right] \\ &= \sum_{m=L_d}^{U_d} \frac{1}{m} \mathbb{P}(\tilde{R}_{\mathcal{T}_{a,\text{rej}}} \geq m, u \in \mathcal{T}_{a,\text{rej}}^m) - \sum_{m'=L_d+1}^{U_d+1} \frac{1}{m'-1} \mathbb{P}(\tilde{R}_{\mathcal{T}_{a,\text{rej}}} \geq m', u \in \mathcal{T}_{a,\text{rej}}^{m'-1}) \\ &= \sum_{m=L_d+1}^{U_d} \left[\frac{1}{m} \mathbb{P}(\tilde{R}_{\mathcal{T}_{a,\text{rej}}} \geq m, u \in \mathcal{T}_{a,\text{rej}}^m) - \frac{1}{m-1} \mathbb{P}(\tilde{R}_{\mathcal{T}_{a,\text{rej}}} \geq m, u \in \mathcal{T}_{a,\text{rej}}^{m-1}) \right] \\ &\quad + \frac{1}{L_d} \mathbb{P}(\tilde{R}_{\mathcal{T}_{a,\text{rej}}} \geq L_d, u \in \mathcal{T}_{a,\text{rej}}^{L_d}) - \frac{1}{U_d} \mathbb{P}(\tilde{R}_{\mathcal{T}_{a,\text{rej}}} \geq U_d+1, u \in \mathcal{T}_{a,\text{rej}}^{U_d}) \\ &\leq \sum_{m=L_d+1}^{U_d} \left[\frac{1}{m} \mathbb{P}(\tilde{R}_{\mathcal{T}_{a,\text{rej}}} \geq m, u \in \mathcal{T}_{a,\text{rej}}^m) - \frac{1}{m-1} \mathbb{P}(\tilde{R}_{\mathcal{T}_{a,\text{rej}}} \geq m, u \in \mathcal{T}_{a,\text{rej}}^{m-1}) \right] \\ &\quad + \frac{1}{L_d} \mathbb{P}(u \in \mathcal{T}_{a,\text{rej}}^{L_d}) \\ &\leq \sum_{m=L_d+1}^{U_d} \frac{1}{m} \mathbb{P}(\tilde{R}_{\mathcal{T}_{a,\text{rej}}} \geq m, u \in \mathcal{T}_{a,\text{rej}}^m \setminus \mathcal{T}_{a,\text{rej}}^{m-1}) + \frac{1}{L_d} \mathbb{P}(u \in \mathcal{T}_{a,\text{rej}}^{L_d}) \\ &\leq \sum_{m=L_d+1}^{U_d} \frac{1}{m} \mathbb{P}(u \in \mathcal{T}_{a,\text{rej}}^m \setminus \mathcal{T}_{a,\text{rej}}^{m-1}) + \frac{1}{L_d} \mathbb{P}(u \in \mathcal{T}_{a,\text{rej}}^{L_d}), \end{aligned} \quad (52)$$

where in the last equality we used the observation $\mathcal{T}_{a,\text{rej}}^{m-1} \subseteq \mathcal{T}_{a,\text{rej}}^m$, since $\alpha_{u,m}$ is increasing in m .

For exposition purposes, we define the shorthand $q_{u,m} = \mathbb{P}(u \in \mathcal{T}_{a,\text{rej}}^m)$ for $u \in \mathcal{T}_a$ and

$m \geq 1$. Then, from the chain of inequalities in (52) we get

$$\begin{aligned}
& \sum_{m=L_d}^{U_d} \frac{1}{m} \mathbb{P}(\tilde{R}_{\mathcal{T}_{a,\text{rej}}} = m, u \in \mathcal{T}_{a,\text{rej}}^m) \\
& \leq \sum_{m=L_d+1}^{U_d} \frac{1}{m} \mathbb{P}(u \in \mathcal{T}_{a,\text{rej}}^m \setminus \mathcal{T}_{a,\text{rej}}^{m-1}) + \frac{1}{L_d} \mathbb{P}(u \in \mathcal{T}_{a,\text{rej}}^{L_d}) \\
& \leq \sum_{m=L_d+1}^{U_d} \frac{1}{m} (q_{u,m} - q_{u,m-1}) + \frac{1}{L_d} q_{u,L_d} \\
& = \sum_{m=L_d}^{U_d} \frac{1}{m} q_{u,m} - \sum_{m=L_d}^{U_d-1} \frac{1}{m+1} q_{u,m} \\
& = \frac{1}{U_d} q_{u,U_d} + \sum_{m=L_d}^{U_d-1} \left(\frac{1}{m} - \frac{1}{m+1} \right) q_{u,m}. \tag{53}
\end{aligned}$$

By deploying (53) in the bound (51), we get

$$\begin{aligned}
& \mathbb{E} \left[\sum_{\mathcal{T}' \in \mathcal{S}(\mathcal{T}_a)} \frac{V_a(\mathcal{T}')}{\tilde{R}_{\mathcal{T}'}} \cdot \mathbb{P}(\mathcal{T}_{a,\text{rej}} = \mathcal{T}' | \mathcal{P}_{\mathcal{T}_a}^c) \right] \\
& \leq \left(\Delta - \frac{1}{\Delta} \right) \sum_{u \in \mathcal{T}_a} \left(\frac{1}{U_d} q_{u,U_d} + \sum_{m=L_d}^{U_d-1} \left(\frac{1}{m} - \frac{1}{m+1} \right) q_{u,m} \right) \\
& = \left(\Delta - \frac{1}{\Delta} \right) \left(\frac{1}{U_d} \sum_{u \in \mathcal{T}_a} q_{u,U_d} + \sum_{m=L_d}^{U_d-1} \frac{1}{m(m+1)} \sum_{u \in \mathcal{T}_a} q_{u,m} \right). \tag{54}
\end{aligned}$$

Our next step is to upper bound $\sum_{u \in \mathcal{T}_a} q_{u,m}$ which is the subject of the following lemma.

Lemma C.1. *For any integer $m \geq 1$ we have*

$$\sum_{u \in \mathcal{T}_a} q_{u,m} \leq \frac{\tilde{\gamma}_{a,m}}{p(\Delta - \frac{1}{\Delta})},$$

where $\tilde{\gamma}_{a,m}$ is given by (28).

The proof of Lemma C.1 is deferred to Section C.1.

By virtue of Lemma C.1 and (54), we have

$$\begin{aligned}
\mathbb{E} \left[\sum_{\mathcal{T}' \in \mathcal{S}(\mathcal{T}_a)} \frac{V_a(\mathcal{T}')}{\tilde{R}_{\mathcal{T}'}} \cdot \mathbb{P}(\mathcal{T}_{a,\text{rej}} = \mathcal{T}' | \mathcal{P}_{\mathcal{T}_a}^c) \right] &\leq \frac{1}{p} \left(\frac{1}{U_d} \tilde{\gamma}_{a,U_d} + \sum_{m=L_d}^{U_d-1} \frac{1}{m(m+1)} \tilde{\gamma}_{a,m} \right) \\
&= \frac{\alpha |\mathcal{L}_a|}{p \tilde{h}_{d,r}} \left(1 + \sum_{m=L_d}^{U_d-1} \frac{1}{m+1} \right) \\
&= \frac{\alpha |\mathcal{L}_a|}{p \tilde{h}_{d,r}} \left(1 + \sum_{m=L_d+1}^{U_d} \frac{1}{m} \right) \\
&= \frac{\alpha |\mathcal{L}_a|}{p}. \tag{55}
\end{aligned}$$

C.1 Proof of Lemma C.1

Since $a \in \mathcal{B}^*$, any node $u \in \mathcal{T}_a$ is a true null and hence it has a super uniform p -value, i.e. for any $x \in [0, 1]$ we have $\mathbb{P}(p_u \leq x) \leq x$. In addition, by our assumption the null p -values are independent and if a node u is rejected so are the nodes on the path from node a to it. Therefore,

$$q_{u,m} = \mathbb{P}(u \in \mathcal{T}_{a,\text{rej}}^m) \leq \tilde{\alpha}_{a,m}^{\text{depth}(u) - \text{depth}(a) + 1}. \tag{56}$$

Here we used the fact that the rejection thresholds in $\mathcal{T}_{a,\text{rej}}^m$ are set to $\tilde{\alpha}_{a,m}$.

Also, since the node degrees in \mathcal{T} are at most Δ , the number of nodes in subtree \mathcal{T}_a that are depth d of the tree \mathcal{T} is at most $\Delta^{d - \text{depth}(a)}$. We therefore have

$$\begin{aligned}
\sum_{u \in \mathcal{T}_a} q_{u,m} &\leq \sum_{d=\text{depth}(a)}^D \Delta^{d - \text{depth}(a)} \tilde{\alpha}_{a,m}^{d - \text{depth}(a) + 1} \\
&\leq \sum_{d=1}^{\infty} \Delta^{d-1} \tilde{\alpha}_{a,m}^d \\
&= \frac{1}{\Delta} \frac{\Delta \tilde{\alpha}_{a,m}}{1 - \Delta \tilde{\alpha}_{a,m}} \\
&= \frac{\tilde{\gamma}_{a,m}}{p(\Delta - \frac{1}{\Delta})}, \tag{57}
\end{aligned}$$

which completes the proof.

D Some useful lemmas

Lemma D.1. *Consider a tree \mathcal{T} with maximum degree Δ . Denote by \mathcal{L} the set of leaf nodes in \mathcal{T} . We then have*

$$|\mathcal{L}| \leq \frac{(\Delta - 1)|\mathcal{T}| + 1}{\Delta},$$

where $|\mathcal{T}|$ denotes the number of nodes in \mathcal{T} .

Proof. Recall that the degree of a node u is the number of its children in the tree. The leaves are of zero degree and the other nodes are of maximum degree Δ . Therefore,

$$(|\mathcal{T}| - p)\Delta \geq \sum_{u \in \mathcal{T}} \deg_{\mathcal{T}}(u) = |\mathcal{T}| - 1.$$

By rearranging the terms we get

$$p \leq \frac{(\Delta - 1) \cdot |\mathcal{T}| + 1}{\Delta}.$$

□

Lemma D.2. Consider a tree \mathcal{T} with maximum degree Δ . For \mathcal{T}' , a subtree of \mathcal{T} , define

$$V(\mathcal{T}') = \sum_{u \in \mathcal{T}'} (\deg_{\mathcal{T}}(u) - \deg_{\mathcal{T}'}(u)) - 1.$$

We then have the following bound on $V(\mathcal{T}')$:

$$V(\mathcal{T}') \leq \frac{(\Delta^2 - 1) \cdot |\mathcal{T}'| + 1}{\Delta} - 1 \leq \left(\Delta - \frac{1}{\Delta} \right) |\mathcal{T}'|,$$

where $|\mathcal{T}'|$ denotes the number of nodes in \mathcal{T}' .

Proof. If node $u \in \mathcal{T}'$ is not a leaf of \mathcal{T}' , we have $\deg_{\mathcal{T}'}(u) \geq 1$ and so

$$\deg_{\mathcal{T}}(u) - \deg_{\mathcal{T}'}(u) \leq \deg_{\mathcal{T}}(u) - 1 \leq \Delta - 1.$$

If $u \in \mathcal{T}'$ is a leaf of \mathcal{T}' , we have

$$\deg_{\mathcal{T}}(u) - \deg_{\mathcal{T}'}(u) = \deg_{\mathcal{T}}(u) \leq \Delta.$$

We therefore have

$$\begin{aligned} V(\mathcal{T}') &= \sum_{u \in \mathcal{T}'} (\deg_{\mathcal{T}}(u) - \deg_{\mathcal{T}'}(u)) - 1 \\ &\leq |\mathcal{L}_{\mathcal{T}'}| \cdot \Delta + (|\mathcal{T}'| - |\mathcal{L}_{\mathcal{T}'}|)(\Delta - 1) - 1 \\ &= |\mathcal{T}'| \cdot (\Delta - 1) + |\mathcal{L}_{\mathcal{T}'}| - 1 \\ &\leq \frac{(\Delta^2 - 1) \cdot |\mathcal{T}'| + 1}{\Delta} - 1 \\ &\leq \left(\Delta - \frac{1}{\Delta} \right) |\mathcal{T}'|, \end{aligned} \tag{1}$$

where the second inequality follows from Lemma D.1. □

E Data generating process for regression simulation

We first form a balanced 3-regular tree with $p = 243$ leaves. We express the tree by a binary matrix $\mathbf{A} \in \{0, 1\}^{p \times |\mathcal{T}|}$ with rows corresponding to features and columns corresponding to nodes. Each entry $A_{ju} = 1$ if node u is an ancestor of leaf j or if $u = j$, and $A_{ju} = 0$ otherwise. For a given K , we cut the tree into K subtrees. The roots of the subtrees form \mathcal{B}^* . We want to set the coefficients corresponding to the leaves within each subtree to the same value. To achieve this, we generate a vector of length K , denoted as $\tilde{\boldsymbol{\theta}}^*$, with the first $(1 - \beta)K$ elements set to 0; the other βK elements of $\tilde{\boldsymbol{\theta}}^*$ are independently drawn from $\mathcal{N}(0, 0.5^2)$. Then we set $\boldsymbol{\theta}^* = \mathbf{A}_{\mathcal{B}^*} \tilde{\boldsymbol{\theta}}^*$, where $\mathbf{A}_{\mathcal{B}^*}$ is matrix \mathbf{A} restricted to columns that correspond to the nodes in \mathcal{B}^* . Note that the columns of $\mathbf{A}_{\mathcal{B}^*}$ have disjoint supports as no two nodes in \mathcal{B}^* can share a same descendant. Parameter β controls the sparsity of $\tilde{\boldsymbol{\theta}}^*$, and therefore sparsity of $\boldsymbol{\theta}^*$.

To simulate a setting with rare feature, we consider a design matrix $\mathbf{X} := \tilde{\mathbf{X}} \odot \mathbf{W} \in \mathbb{R}^{n \times p}$ from a Bernoulli-Gaussian distribution. The entries \tilde{X}_{ij} are generated i.i.d from standard normal distribution. The entries W_{ij} are drawn i.i.d from Bernoulli(ρ). The Bernoulli parameter ρ determines the level of rareness in the design matrix. Also \odot represents the entry-wise product of two matrices. Finally, the high-dimensional linear model is generated by

$$\mathbf{y} = \mathbf{X}\boldsymbol{\theta}^* + \boldsymbol{\varepsilon}, \quad \boldsymbol{\varepsilon} \sim \mathcal{N}(\mathbf{0}, \sigma^2 \mathbf{I}_n), \quad (58)$$

where $\sigma = c \frac{\|\mathbf{X}\boldsymbol{\theta}^*\|_2}{\sqrt{n}}$. We fix the parameters as $n = 100, p = 243, \beta = 0.6, \rho = 0.2, \sigma = 0.6$, and vary K from 21 to 93.

F Stocks data

Table 1 shows the achieved aggregation result.

Table 1: The table shows 40 clusters that are aggregated by our procedure. The rightmost column is the mean log-volatility. The column Company/Number of Companies shows how many companies are in each cluster (or the name of the company when there is only one). The columns from Sector to Industry National show the classification of the clusters that are selected.

Sector	Subsector	Industry Group	Industry	Industry National	Company/Number of Companies	Mean
Agriculture, Forestry, Fishing and Hunting	Mining, Quarrying, and Oil and Gas Extraction	Utilities	Construction	Manufacturing I	5	-7.69
					63	-6.51
					28	-8.4
					45	-7.55
					73	-8.03
					576	-7.48
					75	-7.62
					75	-7.56
					34	-7.5
					44	-7.81
Manufacturing II	Wholesale Trade	Retail Trade I	Retail Trade II	Transportation	3	-8.31
					3	-8.31
					261	-7.5
					50	-7.34
					77	-7.55
					57	-7.65
					12	-7.38
					41	-7.36
					16	-7.75
					52	-7.86
Manufacturing II	Other Services (except Public Administration)	Nonclassifiable Establishments	Wood Product Manufacturing	Paper Manufacturing	6	-8.08
					9	-7.28
					6	-7.55
					19	-8.14
					4	-7.91
					16	-7.93
					17	-7.65
					11	-7.44
					28	-7.18
					6	-7.91
Manufacturing II	Chemical Manufacturing	Basic Chemical Manufacturing	Resin, Synthetic Rubber, and Artificial and Synthetic Fibers and Filaments Manufacturing	Pesticide, Fertilizer, and Other Agricultural Chemical Manufacturing	6	-7.14
					299	-6.37
					6	-8.06
					14	-8.18
					5	-8.35
					64	-7.95
					87	-8.3
					306	-7.64
					32	-7.67
					9	-7.59
Finance and Insurance	Credit Intermediation and Related Activities	Funds, Trusts, and Other Financial Vehicles	Insurance Carriers and Related Activities	Depository Credit Intermediation	MANHATTAN BRIDGE CAPITAL INC	-7.64
					306	-8.27
					32	-7.67
					9	-7.59
					32	-7.67
					9	-7.59
					32	-7.67
					9	-7.59
					32	-7.67
					9	-7.59

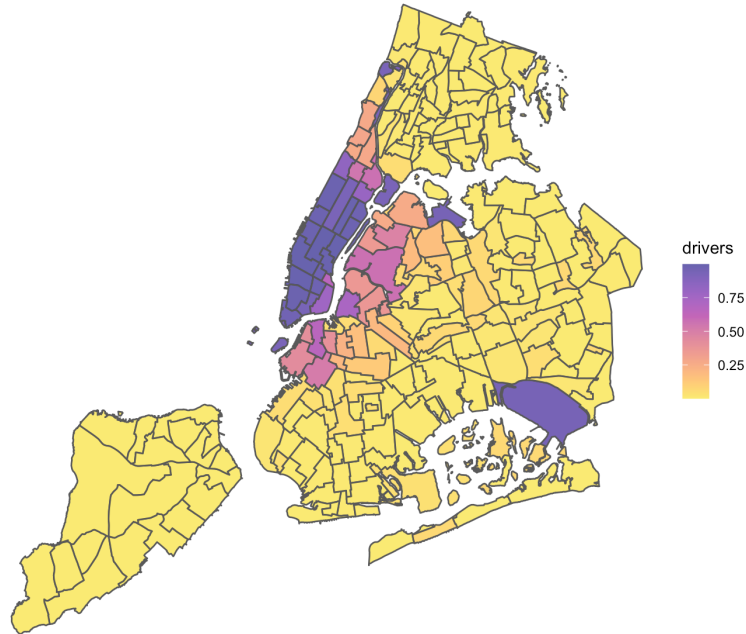


Figure 10: *Map of neighborhoods colored with percentage of drivers who have started a trip from there. Most neighborhoods have fewer than 10% of the drivers starting their trips there in the month of December 2013.*

G NYC taxi data

The availability of taxis is not uniformly distributed across the city (see Figure 10), and \mathbf{X} is a highly sparse matrix: Most areas had fewer than 10% of the drivers starting their trips there during that month, and in fact 109 out of the 194 neighborhoods have seen less than 1% of the drivers.

We study how the aggregation results vary with sample size. To do so, we randomly subset the original dataset to different sizes, and perform the above-mentioned procedure on each sample. The number of achieved groups for each sample size is shown in Table 2. As expected, reduced sample sizes leads to fewer rejections and therefore fewer aggregated groups.

G.1 FSR with synthetic data

To directly evaluate the aggregation recovery performance of HAT, we create a synthetic response based on the tree structure \mathcal{T} constructed by the neighborhoods, as well as the observed trip counts data \mathbf{X} . In addition, we take the aggregation result and fitted coefficients from Section 6.2.1 as the true aggregation and true vector θ^* . We simulate the response 100 times independently according to (58) with $\sigma = 15$. We use the same debiased method to calculate the node-wise p -values and perform our testing procedure with target

Table 2: *Achieved number of groups with decaying sample size.*

Sample Size	p	Number of Groups
$n = 32704$	194	44
$n/2 = 16352$	194	42
$n/4 = 8176$	194	29
$n/8 = 4088$	194	29
$n/16 = 2044$	194	18
$n/32 = 1022$	194	12

Table 3: *Achieved FSR and average power by our algorithm with synthetic data where noise level is $\sigma = 15$.*

Target Level	FSR	Average Power
0.01	0.000	0.547
0.02	0.000	0.560
0.05	0.000	0.577
0.10	0.001	0.593
0.20	0.003	0.608
0.30	0.003	0.620
0.40	0.004	0.626
0.50	0.005	0.632

FSR levels varying from $\alpha = 0.01$ to $\alpha = 0.3$. We compare the aggregation results with the true aggregation and compute FSR and average power over the 100 runs. The results are shown in Table 3.

References

- Benjamini, Y. & Hochberg, Y. (1995), ‘Controlling the false discovery rate: A practical and powerful approach to multiple testing’, *Journal of the Royal Statistical Society. Series B (Methodological)* **57**(1), 289–300.
- Bien, J. (2016), ‘The simulator: an engine to streamline simulations’, *arXiv preprint arXiv:1607.00021* .
- Bien, J., Yan, X., Simpson, L. & Müller, C. L. (2021), ‘Tree-aggregated predictive modeling of microbiome data’, *Scientific Reports* **11**(1), 1–13.
- Blanchard, G. & Roquain, E. (2008), ‘Two simple sufficient conditions for fdr control’, *Electronic Journal of Statistics* **2**(0), 963–992.
- Bogomolov, M., Peterson, C. B., Benjamini, Y. & Sabatti, C. (2017), ‘Testing hypotheses on a tree: new error rates and controlling strategies’, *arXiv preprint arXiv:1705.07529* .

- Cai, T., Cai, T. & Guo, Z. (2019a), ‘Individualized treatment selection: An optimal hypothesis testing approach in high-dimensional models’, *arXiv preprint arXiv:1904.12891* .
- Cai, T., Cai, T. & Guo, Z. (2019b), ‘Optimal statistical inference for individualized treatment effects in high-dimensional models’, *arXiv preprint arXiv:1904.12891 (To appear in Journal of the Royal Statistical Society: Series B)* .
- Cai, T. T., Guo, Z. et al. (2017), ‘Confidence intervals for high-dimensional linear regression: Minimax rates and adaptivity’, *The Annals of statistics* **45**(2), 615–646.
- Compustat Industrial - Annual Data (2015-2019). Available: Standard & Poor’s Compustat [01/26/2021]. Retrieved from Wharton Research Data Service.
- CRSP Stocks (2015-2019). Available: Center For Research in Security Prices. Graduate School of Business. University of Chicago [01/26/2021]. Retrieved from Wharton Research Data Service.
- Guo, Z., Renaux, C., Bühlmann, P. & Cai, T. T. (2019), ‘Group inference in high dimensions with applications to hierarchical testing’, *arXiv preprint arXiv:1909.01503* .
- Heller, R., Chatterjee, N., Krieger, A. & Shi, J. (2018), ‘Post-selection inference following aggregate level hypothesis testing in large-scale genomic data’, *Journal of the American Statistical Association* **113**(524), 1770–1783.
- Javanmard, A. & Lee, J. D. (2020), ‘A flexible framework for hypothesis testing in high dimensions’, *Journal of the Royal Statistical Society: Series B (Statistical Methodology)* **82**(3), 685–718.
- Javanmard, A. & Montanari, A. (2014), ‘Confidence intervals and hypothesis testing for high-dimensional regression’, *The Journal of Machine Learning Research* **15**(1), 2869–2909.
- Javanmard, A. & Montanari, A. (2018a), ‘Debiasing the lasso: Optimal sample size for gaussian designs’, *The Annals of Statistics* **46**(6A), 2593–2622.
- Javanmard, A. & Montanari, A. (2018b), ‘Online rules for control of false discovery rate and false discovery exceedance’, *The Annals of statistics* **46**(2), 526–554.
- Katsevich, E. & Sabatti, C. (2019), ‘Multilayer knockoff filter: Controlled variable selection at multiple resolutions’, *The annals of applied statistics* **13**(1), 1.
- Lynch, G. & Guo, W. (2016), ‘On procedures controlling the fdr for testing hierarchically ordered hypotheses’, *arXiv preprint arXiv:1612.04467* .
- Martens, M. & van Dijk, D. (2007), ‘Measuring volatility with the realized range’, *Journal of Econometrics* **138**(1), 181–207. 50th Anniversary Econometric Institute.

- Meinshausen, N. (2008), ‘Hierarchical testing of variable importance’, *Biometrika* **95**(2), 265–278.
- NYC Planning (2020). Available: ”Neighborhood Tabulation Areas (Formerly ”Neighborhood Projection Areas”)”. Retrieved from September 22, 2020.
- Parkinson, M. (1980), ‘The extreme value method for estimating the variance of the rate of return’, *The Journal of Business* **53**(1), 61–65.
- Ramdas, A., Chen, J., Wainwright, M. J. & Jordan, M. I. (2017), ‘Dagger: A sequential algorithm for fdr control on dags’, *ArXiv* **abs/1709.10250**.
- Seber, G. A. F. & Lee, A. J. (2012), *Linear regression analysis*, Wiley.
- Simes, R. J. (1986), ‘An improved bonferroni procedure for multiple tests of significance’, *Biometrika* **73**(3), 751–754.
- Sun, T. & Zhang, C.-H. (2012), ‘Scaled sparse linear regression’, *Biometrika* **99**(4), 879–898.
- Tibshirani, R. (1996), ‘Regression shrinkage and selection via the lasso’, *Journal of the Royal Statistical Society: Series B (Methodological)* **58**(1), 267–288.
- US OMB (2017), ‘North american industry classification system’, *Executive Office of the President; Office of Management and Budget*.
URL: https://www.census.gov/naics/reference_files_tools/2017_NAICS_Manual.pdf
- US OMB (2018), ‘Standard occupational classification manual’, *Executive Office of the President; Office of Management and Budget*.
URL: https://www.bls.gov/soc/2018/soc_2018_manual.pdf
- van de Geer, S., Bühlmann, P., Ritov, Y. & Dezeure, R. (2014), ‘On asymptotically optimal confidence regions and tests for high-dimensional models’, *The Annals of Statistics* **42**(3), 1166–1202.
- Wilms, I. & Bien, J. (2021), ‘Tree-based node aggregation in sparse graphical models’, *arXiv preprint arXiv:2101.12503*.
- Yan, X. & Bien, J. (2020), ‘Rare feature selection in high dimensions’, *Journal of the American Statistical Association* **0**(0), 1–14.
- Yan, X. & Bien, J. (n.d.), *rare: Linear Model with Tree-Based Lasso Regularization for Rare Features*. R package version 0.1.0.
URL: <https://github.com/yanxht/rare>
- Yekutieli, D. (2008), ‘Hierarchical false discovery rate-controlling methodology’, *Journal of the American Statistical Association* **103**(481), 309–316.

Zhang, C.-H. & Zhang, S. S. (2014), ‘Confidence intervals for low dimensional parameters in high dimensional linear models’, *Journal of the Royal Statistical Society: Series B (Statistical Methodology)* **76**(1), 217–242.